

SPRAY PROCESSABLE AMBIPOLAR BENZOTRIAZOLE BEARING
ELECTROCHROMIC POLYMERS
WITH MULTI-COLORED AND TRANSMISSIVE STATES

A THESIS SUBMITTED TO
THE GRADUATE SCHOOL OF NATURAL AND APPLIED SCIENCES
OF
MIDDLE EAST TECHNICAL UNIVERSITY

BY

GÖNÜL HIZALAN

IN PARTIAL FULFILLMENT OF THE REQUIREMENTS
FOR
THE DEGREE OF MASTER OF SCIENCE
IN
CHEMISTRY

SEPTEMBER 2011

Approval of the thesis:

**SPRAY PROCESSABLE AMBIPOLAR BENZOTRIAZOLE BEARING
ELECTROCHROMIC POLYMERS
WITH MULTI-COLORED AND TRANSMISSIVE STATES**

submitted by **GÖNÜL HIZALAN** in partial fulfillment of the requirements for the degree of **Master of Science in Chemistry Department, Middle East Technical University** by,

Prof. Dr. Canan Özgen
Dean, Graduate School of **Natural and Applied Sciences**

Prof. Dr. İlker Özkan
Head of Department, **Chemistry**

Prof. Dr. Levent Toppare
Supervisor, **Chemistry Dept., METU**

Examining Committee Members:

Prof. Dr. Levent Toppare
Chemistry Dept., METU

Assoc. Prof. Dr. Yasemin Arslan Udum
Chemistry Dept., Gazi University

Assist. Prof. Dr. Ali Çırpan
Chemistry Dept., METU

Assist. Prof. Dr. İrem Erel
Chemistry Dept., METU

Assist. Prof. Dr. Ertuğrul Şahmetlioğlu
Chemistry Dept., Niğde University

Date: 06.09.2011

I hereby declare that all information in this document has been obtained and presented in accordance with academic rules and ethical conduct. I also declare that, as required by these rules and conduct, I have fully cited and referenced all material and results that are not original to this work.

Name, Last name: GÖNÜL HIZALAN

Signature

ABSTRACT

SPRAY PROCESSABLE AMBIPOLAR BENZOTRIAZOLE BEARING ELECTROCHROMIC POLYMERS WITH MULTI-COLORED AND TRANSMISSIVE STATES

Hızalan, Gönül
M.Sc., Department of Chemistry
Supervisor: Prof. Dr. Levent Toppare

September 2011, 57 pages

The interest towards organic semi-conductors increased due to their tunable band gaps, redox properties, processability and low cost in the field of conducting polymers. Electrochromic materials have the ability to change color by altering their redox state. In the context of low cost flexible display device technology, requirements can be fulfilled with accessible multi-colored electrochromic polymers. In this study, we report the chemical synthesis and electrochromic properties of two spray processable, ambipolar, fluorescent and multi-color to transmissive electrochromic polymers. The electrochromic properties of these polymers were examined by cyclic voltammetry, spectroelectrochemistry, kinetic studies. Polymers, PTBTPh and PTBTTh, have multi-colored oxidation states and easily accessible n-doped states, which allowed us to achieve transmissive films in a low working potential. Electrochemical and spectral results showed that both polymers are potential materials for electrochromic display devices.

Keywords: Electrochromism, Donor-acceptor, Multichromic polymers, Benzotriazole

ÖZ

SPREY KAPLAMA YAPILABİLEN, AMBİPOLAR, MULTİ-ELEKTROKROMİK VE SAYDAM HALLERE SAHİP BENZOTRIAZOL İÇEREN ELEKTROKROMİK POLİMERLER

Hızalan, Gönül
Yüksek Lisans, Kimya Bölümü
Tez yöneticisi: Prof. Dr. Levent Toppare

Eylül 2011, 57 sayfa

Değişebilen bant aralıkları, yükseltgenme ve indirgenme özellikleri, işlenebilirlikleri ve ucuzlukları nedeniyle ilteken polimerler alanında organik yarı iletkenlere olan ilgi artmıştır. Elektrokromik malzemeleri yükseltgeyerek ve indiregeyerek renklerini değiştirmemiz mümkündür. Çok renkli elektrokromik malzemeler ucuz, esnek görüntü teknolojisinin gerekliliklerini yerine getirebilmektedirler. Bu çalışmada, spreycaplama yapabilen, ambipolar, floresan ve birçok renkten saydam hale geçebilen elektrokromik iki polimer kimyasal yollarla sentezlenmiştir ve elektrokimyasal özellikleri incelenmiştir. Bu polimerlerin elektrokimyasal özellikleri dönüşümlü voltametre, spektroeletrokimya ve kinetik çalışmalarla incelenmiştir. Polimerler, PTBTPH ve PTBTTh, oksitlendiklerinde birden fazla renk verebilmeleri ve kolayca n tipi katkılanabilir olmaları, düşük potansiyellerde saydam filmler elde etmemizi sağlamıştır. Elektrokimyasal ve spectral sonuçlara göre, bu polimerlerin elektrokromik görüntü aparatlarında kullanılması mümkündür.

Anahtar kelimeler: Elektrokromizm, Donor akseptör, Multikromik polimerler, Benzotriazol

To My Family

ACKNOWLEDGEMENTS

I am grateful to my supervisor Prof. Dr. Levent Toppare for his guidance, support, advice, criticism and for helping me in many ways.

I would like to thank to TUBİTAK (Turkish Scientific and Technical Research Council) for the scholarship.

I owe special thanks to Simge Tarku and Abidin Balan for their endless helps in organic synthesis besides their kind friendship.

I would like to thank to Yasemin Arslan Udum and Ali ırpan for their valuable discussions.

I would like to thank to Derya Baran for her help in the electrochemical characterizations.

Many thanks to Gzde ktem, Doėukan Apaydın, Hava Akpınar for their friendship and coffee breaks.

Thanks go to all Toppare Research Group members for their cooperation.

Special thanks to Grkem ŐimŐek for her friendship and support.

I would like to thank to Kubilay Kaan zsoy for his patience, understanding, help and love.

Words fail to express my eternal gratitude to my family for believing in me and giving me endless support.

TABLE OF CONTENTS

ABSTRACT	iv
ÖZ	v
ACKNOWLEDGEMENTS	vii
TABLE OF CONTENTS	viii
LIST OF TABLES	x
LIST OF FIGURES	xi
LIST OF ABBREVIATIONS	xiv
CHAPTERS	1
1. INTRODUCTION.....	1
1.1 Conducting Polymers.....	1
1.2 Band Theory.....	5
1.3 Doping Process	7
1.4 Chromism.....	7
1.4.1 Electrochromism	8
1.5 Polymerization Methods	11
1.5.1 Electrochemical Polymerization	11
1.5.2 Chemical Polymerization.....	13
1.6 Factors Affecting Band gap	14
1.7 Aim of This Work	19
2. EXPERIMENTAL	20
2.1 Materials.....	20
2.2 Methods.....	20
2.3 Equipment	21

2.4 Procedure	22
2.4.1 Synthesis of 2-dodecylbenzotriazole.....	22
2.4.2 Synthesis of 4,7-dibromo-2-dodecylbenzotriazole	23
2.4.4 Synthesis of 2,5-bis(tributylstannyl)thiophene	24
2.4.5 Synthesis of 2-dodecyl-4,7-di(thiophen-2-yl)-2H-benzo[d][1,2,3]triazole	25
2.4.6 Synthesis of 4,7-bis(5-bromothiophen-2-yl)-2dodecyl2Hbenzo[d][1,2,3] triazole.....	26
2.4.7 Synthesis of PTBTPh.....	27
2.4.8 Synthesis of PTBTTh.....	28
2.5 Characterization of Conducting Polymers	29
2.5.1 Cyclic Voltammetry (CV).....	29
2.5.2 Spectroelectrochemistry	30
2.5.3 Kinetic Studies	31
3. RESULTS AND DISCUSSION	33
3.1 Polymer Synthesis.....	33
3.2 Electrochemistry	34
3.2.1 Electrochemistry of PTBTPh	34
3.2.1 Electrochemistry of PTBTTh.....	35
3.3 Spectroelectrochemistry	37
3.3.1 Spectroelectrochemistry of PTBTPh	38
3.3.2 Spectroelectrochemistry of PTBTTh	39
3.4 Absorbance and Photoluminescence Studies of PTBTPh and PTBTTh	42
3.4 Kinetic Properties of PTBTPh and PTBTTh	43
4. CONCLUSION.....	46
REFERENCES.....	47
APPENDIX.....	51

LIST OF TABLES

TABLES

Table 3.1 Electrochemical results, HOMO-LUMO energies and band gap values for PTBTPh and PTBTTh.....	37
Table 3.2 Spectroscopic and optical results for polymers PTBTPh, PTBTTh, PTBTe (electrochemically synthesized) and PTBTc (chemically synthesized). * Data obtained from 39b	45

LIST OF FIGURES

FIGURES

Figure 1.1 Polymerization of acetylene to trans- polyacetylene	1
Figure 1.2 Doping mechanism of polyacetylene.....	2
Figure 1.3 Conductivity ranges of insulators, semiconductors and metals [2]	3
Figure 1. 4 Structures of common conducting polymers. (1) polyacetylene, (2) polythiophene (3) polyfuran, (4) polypyrrole, (5) poly3-hexylthiophene, (6) poly(3,4-ethylenedioxy-thiophene), (7) poly(3,4-propylenedioxy-thiophene), (8) poly(p-phenylene), (9) polyaniline, (10) poly(p-phenylenevinylene), (11) poly(thienylenevinylene), (12) polycarbazole.....	4
Figure 1. 5 Band diagrams for insulators, semiconductors and metals.....	6
Figure 1. 6 Generation of band structure for polythiophene [12]	7
Figure 1 .7 Redox switching mechanism of viologens	9
Figure 1.8 Electrochemical polymerization mechanism of thiophene	12
Figure 1.9 Synthesis of polythiophene via a) metal catalyzed coupling and b) chemical oxidation.....	13
Figure 1.10 Overview of methods for the modification of band gap [26]	14
Figure 1.11 a) Illustration of degenerate ground state of polyacetylene, b) Illustration of non- degenerate ground state of polythiophene [28]	15
Figure 1.12 Evolution from polyacetylene to poly(BEDOT-Pyr)[29,30].....	16
Figure 1.13 Schematic representation of the donor-acceptor approach to narrow band gap conjugated polymers [41]	18
Figure 1.14 Structure of TBT and synthesis of PTBT	19
Figure 2.1 Synthesis of 2-Dodecylbenzotriazole	22
Figure 2.2 Synthesis of 4,7-Dibromo-2-dodecylbenzotriazole	23
Figure 2.3 Synthesis of Tributyl(thiophen-2yl)stanne	24
Figure 2.4 Synthesis of 2,5-bis(tributylstannyl)thiophene	24

Figure 2.5 Synthesis of 2-Dodecyl-4,7-di(thiophen-2-yl)-2H-benzo[d][1,2,3]triazole	25
Figure 2.6 Synthesis of 4,7-bis(5-bromothiophen-2-yl)-2dodecyl2Hbenzo[d][1,2,3] triazole.....	26
Figure 2.7 Synthesis of PTBTPh.....	27
Figure 2.8 Synthesis of PTBTTh.....	28
Figure 2.9 Demonstration of electrochemistry experiment set up	29
Figure 2.10 (a) Demonstration of applied potential as function of time	30
Figure 2.11 Spectra of a representative conducting polymer.....	31
Figure 2.12 Kinetic study of a representative conducting polymer	32
Figure 3.1 Chemical structures of PTBTPh and PTBTTh	34
Figure 3.2 Cyclic voltammogram of PTBTPh	35
Figure 3.3 Cyclic voltammogram of PTBTTh.....	36
Figure 3.4 Spectroelectrochemistry studies of spray cast films of PTBTPh.....	38
Figure 3.5 Spectroelectrochemistry studies of spray cast films of PTBTTh	39
Figure 3.6 Spray coated PTBTTh (above) and PTBTPh (below) photographs in their neutral and fully oxidized states in 0.1 M TBAPF ₆ /ACN solution and the potentials where the corresponding colors were monitored.	42
Figure 3.7 Solution and film absorbance spectra of PTBTPh and PTBTTh both in thin film form and solution (on the left) and emission spectra of polymer solutions in chloroform.....	43
Figure 3.8 Percent transmittance changes by continuous monitoring at dominant wavelengths during switching between 0.0 V and 1.2 V in 0.1 M TBAPF ₆ / ACN solution.....	44
Figure A.1 ¹ H-NMR spectrum of 2-dodecyl-2H-benzo[d][1,2,3]triazole	51
Figure A.2 ¹ H-NMR spectrum of 4,7-dibromo-2-dodecyl-2H-benzo[d][1,2,3]triazole.....	52
Figure A.3 ¹ H-NMR spectrum of 2,5-bis(tributylstannyl)thiophene.....	53

Figure A.4 ¹ H-NMR spectrum of 2-dodecyl-4,7-di(thiophen-2-yl)-2H-benzo[d][1,2,3]triazole	54
Figure A.5 ¹ H-NMR spectrum of 4,7-bis(5-bromothiophen-2-yl)-2dodecyl-2Hbenzo[d][1,2,3] triazole	55
Figure A.6 ¹ H-NMR spectrum of PTBTP	56
Figure A.7 ¹ H-NMR spectrum of PTBTTh.....	57

LIST OF ABBREVIATIONS

ACN	Acetonitrile
CB	Conduction Band
CP	Conducting Polymer
CV	Cyclic Voltammetry
DCM	Dichloromethane
DA	Donor Acceptor
E_g	Band Gap Energy
HOMO	Highest Occupied Molecular Orbital
ITO	Indium Tin Oxide
OLED	Organic Light Emitting Diode
LUMO	Lowest Unoccupied Molecular Orbital
NMR	Nuclear Magnetic Resonance
PA	Polyacetylene
PBEDOT-CNV	Poly(bis-EDOT)-cyanovinylene
PEDOP	Poly(ethylenedioxy pyrrole)
PEDOT	Poly(ethylenedioxy thiophene)
PTh	Polythiophene
TBAPF₆	Tetrabutylammonium hexafluorophosphate
VB	Valence Band

CHAPTER 1

INTRODUCTION

1.1 Conducting Polymers

Three collaborating scientists Alan J. Heeger, Alan G. MacDiarmid and Hideki Shirakawa were awarded with the Nobel Prize in Chemistry for 2000 for the discovery and development of conductive polymers [1]. They have discovered a new class of polymers which are electrically conductive in their oxidized or reduced states. Polymers are formed by bounding of many identical units like pearls in a necklace. In order a polymer to be electrically conductive it must mimic a metal. Like metals, bonding electrons must be freely mobile and not bound tight to the atoms. One condition for providing this is that the polymer consists of alternate single and double bonds, so called as “conjugated double bonds”. The simplest conjugated polymer is polyacetylene, it is obtained by polymerization of acetylene.

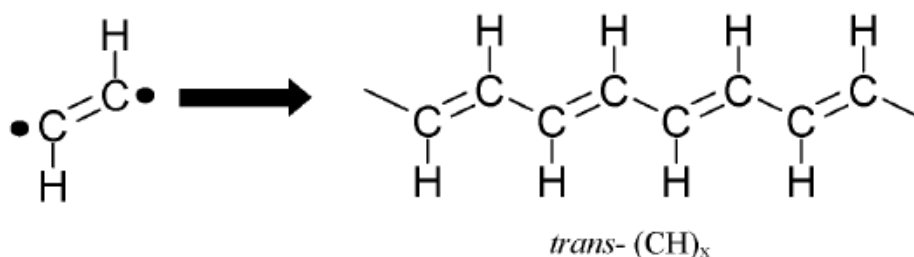


Figure 1.1 Polymerization of acetylene to trans- polyacetylene

Polyacetylene was known as a black powder previous to Shirakawa and co-workers' study. Shirakawa and co-workers synthesized polyacetylene starting with acetylene and using Ziegler-Natta catalyst. Accidentally they used the catalyst one thousand times more than needed and they end up with silvery film formed on the surface of the liquid. After that, the three Nobel Prize Laureates co-operated to investigate the properties of the film formed. Although the appearance of the film is similar to metals, it was not a conductor. They caused the polyacetylene films to react iodine vapor.

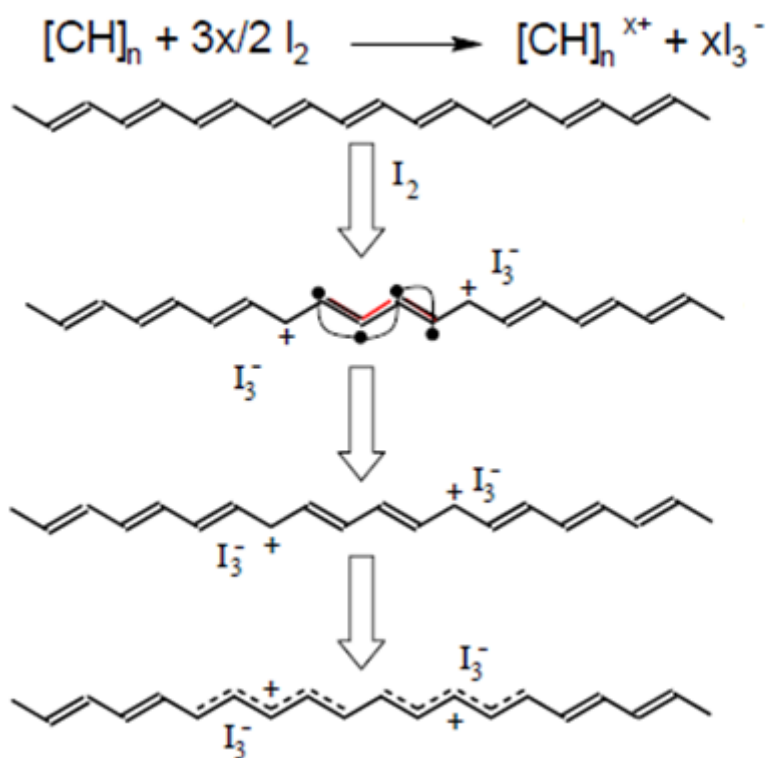


Figure 1.2 Doping mechanism of polyacetylene

Iodine vapor causes oxidation which leads to the removal of the electrons from the polymer chain, formation of "holes" in the form of positive charges that can move along the chain. Treatment with iodine vapor is called "doping". The "doped" form

of polyacetylene had a conductivity of 10^6 Siemens per meter, which was higher than that of any previously known polymer. [1]

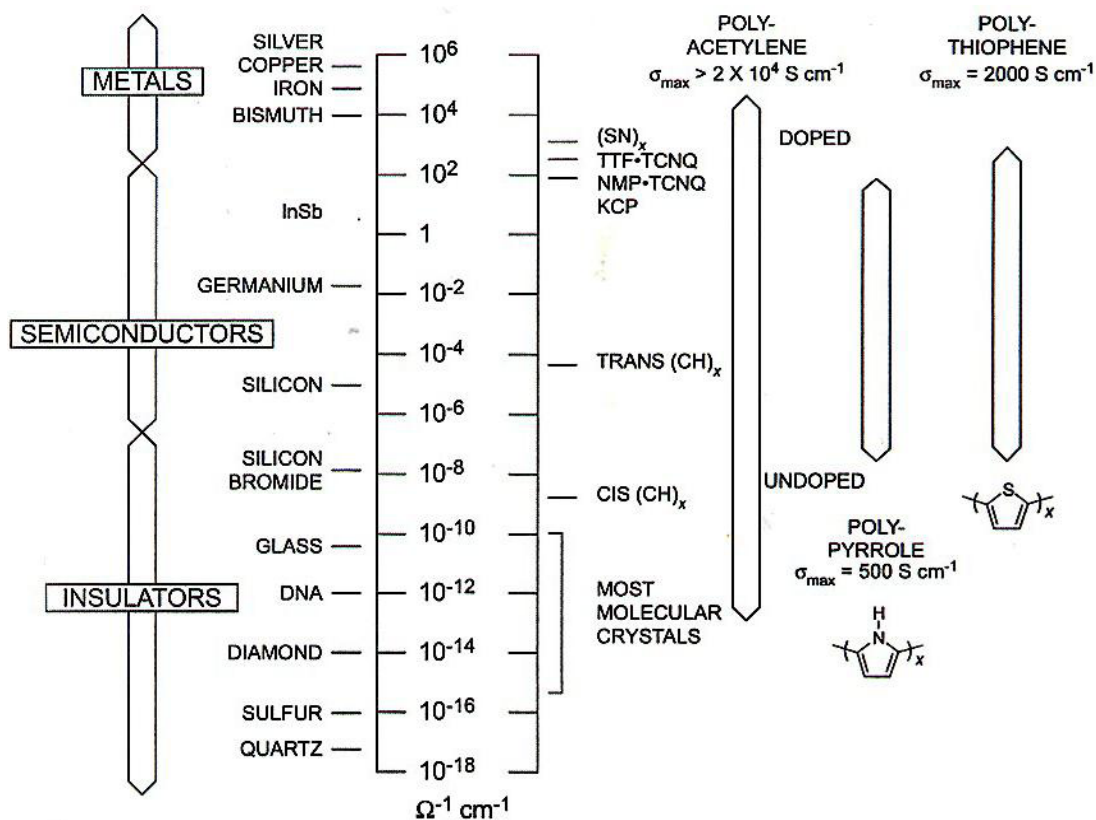


Figure 1.3 Conductivity ranges of insulators, semiconductors and metals [2]

The conductivity of polyacetylene increased by as much as ten million times with this doping process; the more electrons are removed, the higher the degree of doping and the greater the conductivity. Although the high conductivity of PAc opened up the field of “plastic electronics”, it is not convenient for practical purposes since it is insoluble and unstable to air and humidity. These obstacles led scientists to the development of more stable conjugated polymers.

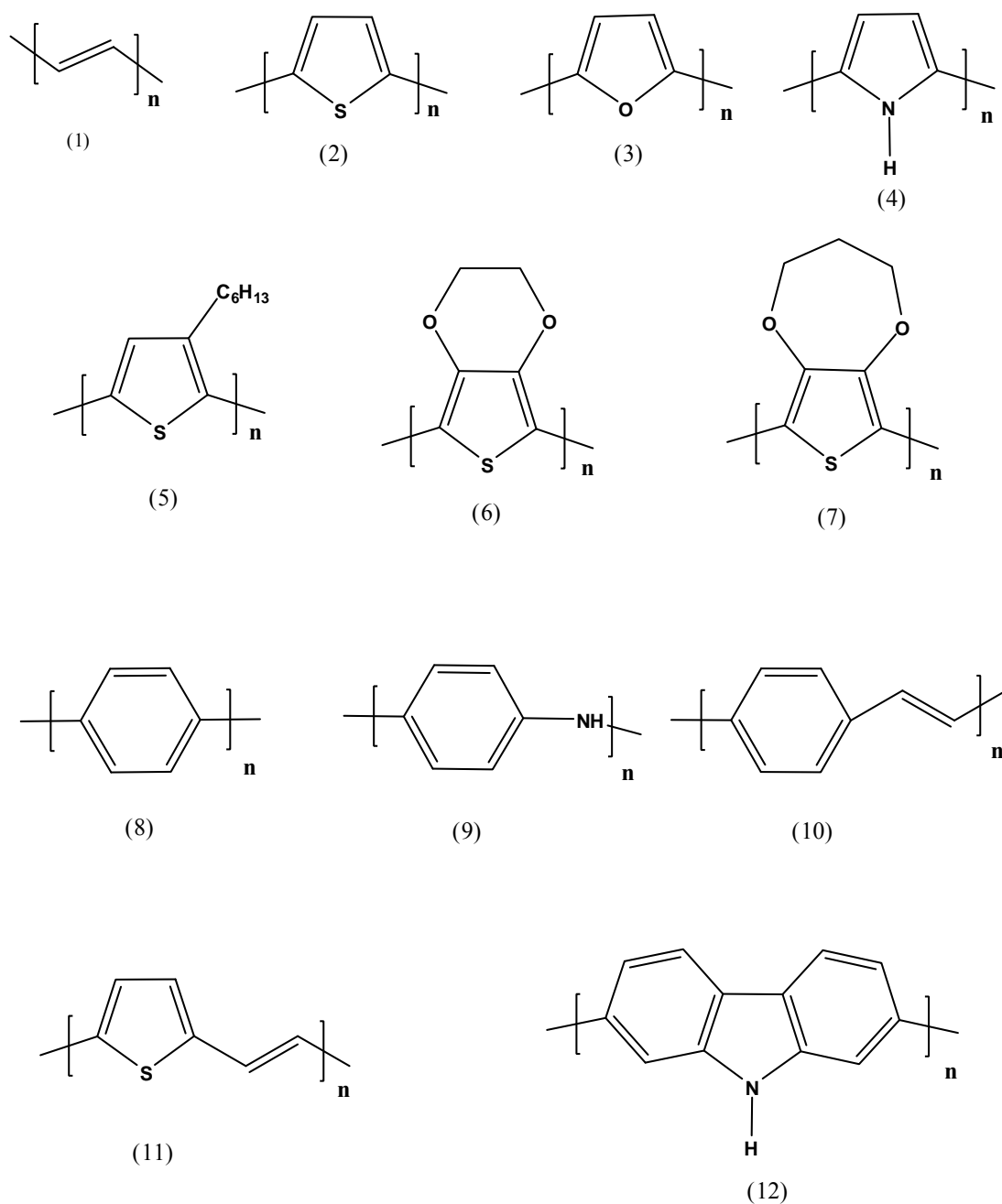


Figure 1. 4 Structures of common conducting polymers. (1) polyacetylene, (2) polythiophene (3) polyfuran, (4) polypyrrole, (5) poly3-hexylthiophene, (6) poly(3,4-ethylenedioxy-thiophene), (7) poly(3,4-propylenedioxy-thiophene), (8) poly(p-phenylene), (9) polyaniline, (10) poly(p-phenylenevinylene), (11) poly(thienylenevinylene), (12) polycarbazole

As in many other cases of science, there were many preliminary studies which precurred to discovery of conducting polymers by Heeger, MacDiarmid and Shirakawa . In 1862, Henry Letheby anodically oxidize aniline and get polyaniline which was conductive and possesses electrochromic property.[3] In the 1970s, it is investigated that poly(sulphur nitride) (SN)_x, which is inorganic explosive polymer was superconductive at very low temperatures (T_c=0.26 K). K. Bechgaard and with D. Jerome discovered super conductor organic compounds at rather high temperatures.(T_c around 10 K) [4].

Combining the electrical properties of semiconductors with the properties of polymers makes these compounds excellent materials for sensors [5,6], active materials for organic solar cells (OPVs) [7], organic light-emitting diodes (OLEDs) [8], organic field effect transistors (OFETs) [9] and electrochromic devices (ECDs) [10,11].

1.2 Band Theory

Band gap is defined as the energy difference between highest occupied molecular orbital (HOMO), also known as valence band and the lowest unoccupied molecular orbital (LUMO), also known as the conduction band. Band gap of conducting polymers can be approximated in two ways. It can also be calculated from the onset of the π - π^* transition in the UV-Vis spectrum. For the ambipolar (both p and n dopable) polymers, it can be calculated from the oxidation and reduction onset values. According to conductivity, conjugated polymers are in the group of semiconductors. Since conduction and valence bands of metals overlapped, metals have zero band gap. On the other hand, for insulators the energy difference between HOMO and LUMO levels are so huge that they have large band gap. In terms of band gap values, conjugated polymers lie in between metals and insulators.

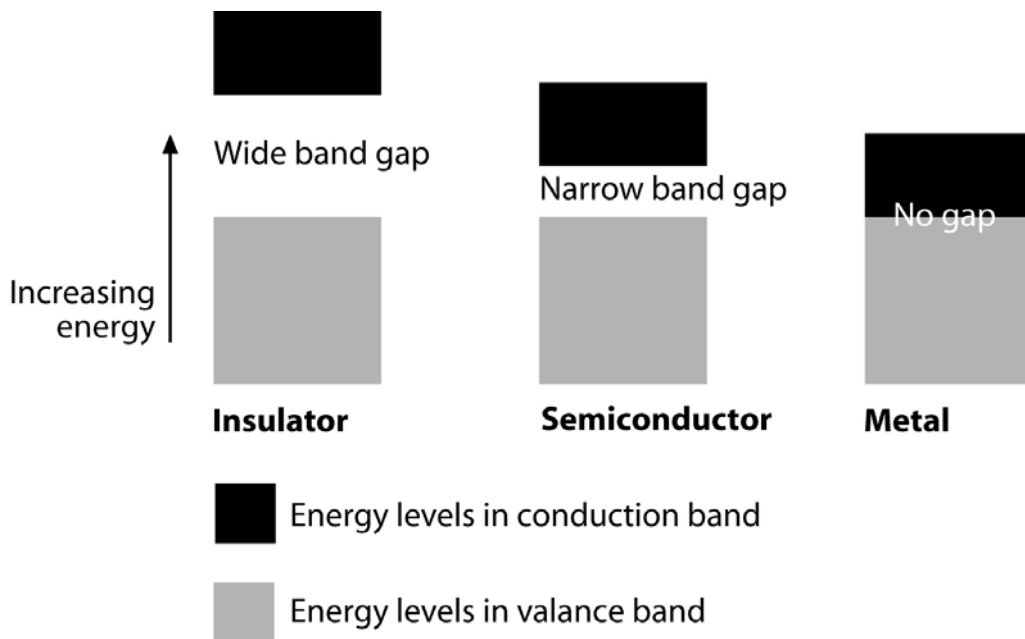


Figure 1.5 Band diagrams for insulators, semiconductors and metals

However, upon doping conjugated polymers may become conductor, due to the formation of interbands between valence and conduction band. Figure 1.6 demonstrates the generation of interbands as the number of repeating units increases. As the conjugation increases, repeating units' π orbitals are overlapping so that there is no more discrete energy levels, continuum band structures are formed.

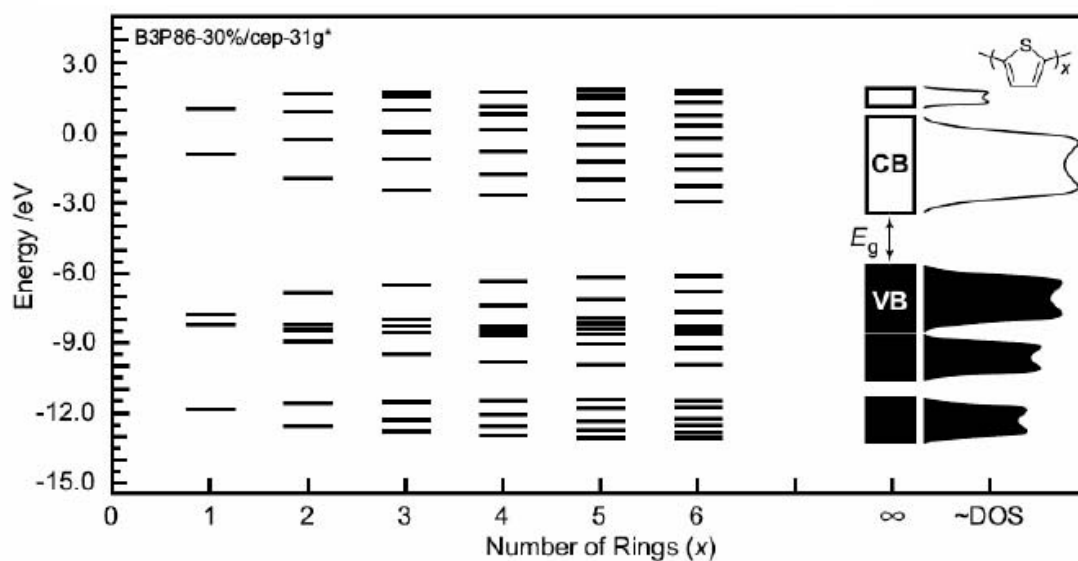


Figure 1. 6 Generation of band structure for polythiophene [12]

1.3 Doping Process

Doping is defined as the injection of charges to the polymer chain. Oxidation process removes an electron from the polymer chain; called p-doping. Reduction process adds an electron to the polymer chain; called n-doping. Since the organic anions are relatively unstable to oxygen and air, n dopable conjugated polymers are rare than the p- dopable ones.

1.4 Chromism

Chromism is defined as the color change of materials upon external stimulus. Reversible color change may be resulted from change in temperature (thermochromism), mechanical effects (piezochromism), solvent (solvatochromism) pH change (halochromism) and electrochemical effects (electrochromism).

1.4.1 Electrochromism

Electrochromism is defined as the reversible change in optical properties of a material upon oxidation or reduction. Important parameters in electrochromic materials are switching times, coloration efficiency, long term stability, contrast ratio and electrochromic memory.

1.4.1.1 Types of Electrochromic Materials

1.4.1.1.1 Metal Oxides

In 1969 electrochromism phenomenon has started with the WO_3 which is a high band gap semiconductor [13]. The oxidation state of tungsten sites in WO_3 is W^{VI} and it is transparent. Upon reduction, blue color is generated due to the formation of W^{V} sites. The generalized process can be written as follows:



M designates the metal cation which can be Li^+ or H^+ [14]. Until now, V, Mo, Nb oxides which are cathodically coloring and Ni, Co, Ir oxides which are anodically coloring, have been studied to investigate their electrochromic behaviors [15].

1.4.1.1.2 Viologens

Viologens are another type of electrochromic materials which are 1,1'-disubstituted-4,4'-bipyridilium salts. Figure 1.7 demonstrates the redox switching mechanism of viologens.

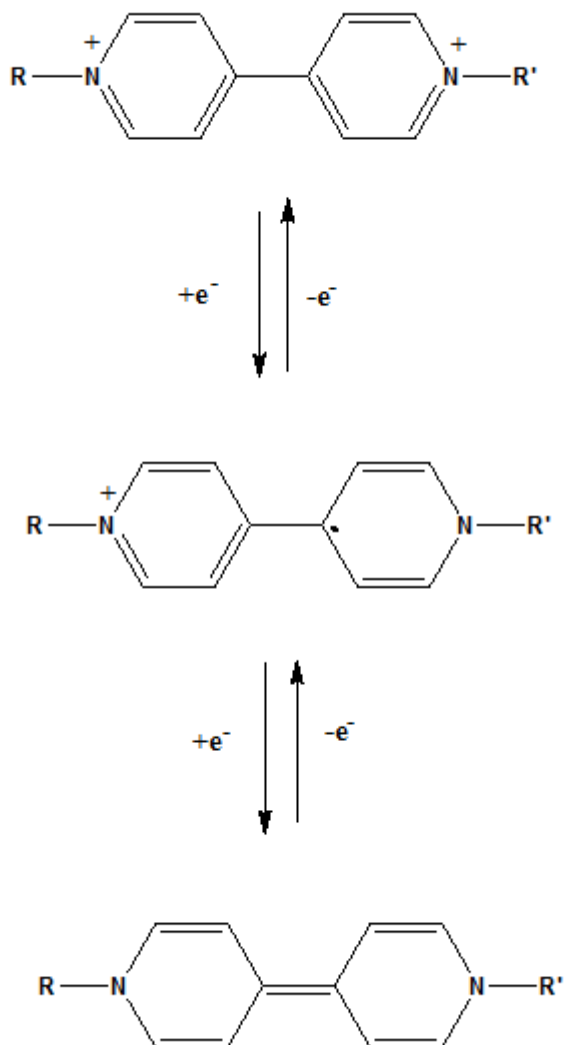


Figure 1 .7 Redox switching mechanism of viologens

By modifying the alkyl group it is possible to obtain viologens switching between different colors. Methyl viologen is the most extensively used viologen derivative, it switches between transmissive state and purple – blue state upon reduction. On the other hand, upon reduction 4- cyanophenyl viologens switches between transmissive state and green state [16].

1.4.1.1.3 Prussian Blue Systems

Prussian blue is iron(III) hexacyanoferrate(II) and it is accidentally formed while scientists were working on oxidation of iron. Partial oxidation of Prussian blue films gives prussian green, whereas full oxidation yields Prussian brown. In addition to this, reduction of prussian blue gives transmissive Prussian white [17].

1.4.1.1.4 Conducting Polymers

Electrochromic polymers (ECPs) reveal a reversible color change upon the application of an appropriate potential. Redox switching results in new optical absorption bands due to simultaneous transport of the electronic charge into the polymer chain. Upon oxidation (loss of electrons) or reduction (gain of electrons), conducting polymers are charge-balanced, namely doped, with counter ions and they adopt a delocalized p-electron band structure [18]. This structural change shifts the optical absorption bands towards the lower energy part of the spectrum. Since the energy gap between HOMO and LUMO levels lies in the visible region, most of the CPs are colored in their neutral, undoped form. If the shift in the absorption is high enough, the polymer film becomes transparent after doping. When more than two redox states, absorbing in the visible, are electrochemically accessible, the ECP may exhibit multi-colors in its different states [15]. This is a result of a high energy absorption of the polaronic states which also tails into the visible region. It is important to remark that although all conjugated polymers have potential to exhibit two colors, only a few show multi-colored states. To date some methodologies, such as copolymerization and structural modifications on the polymer backbone, have been followed in order to achieve multi-colored electrochromic materials.[19] As multi-colored electrochromic homo-polymers, poly(ethylenedioxythiophene) (PEDOT) derivatives like poly(bis-EDOT-pyridopyrazine),[20] poly(ethylenedioxyppyrrrole) (PEDOP) derivatives like N-ethyl substituted poly(3,4-ethylenedioxyppyrrrole),[21] and some thiophene derivatives [22] have been reported.

Moreover, molecular doping of polypyrrole by an electrochromogen (2,20-azino-bis(3-ethylbenzothiazoline -6-sulfonate)) was also utilized as another strategy to achieve multi-color electrochromism [23]. However, the present multi-color electrochromes have some important drawbacks limiting their applications in light-weight and flexible display systems, such as insolubility or lack of a redox achievable transparent state.

Conducting polymers have tremendous advantages over other electrochromics such as attainability of faster response times, higher contrast ratios, color tunability via structural modification and easy processibility (e.g. electrochemical deposition, spin coating and spray coating).

1.5 Polymerization Methods

There are two main polymerization techniques to synthesize conducting polymers, they are electrochemical and chemical polymerization. Via electrochemical ways synthesis of polymer is very quick, whereas chemical polymerization needs more time though it allows large scale production which is important from the point of application.

1.5.1 Electrochemical Polymerization

Electrochemical polymerization takes place on the surface of Indium tin oxide (ITO) coated glass slides with the applied potential inducing oxidation of monomers to polymers. It allows for synthesis of the desired polymer on an electrode's surface that is needed for both electrochemical and optical studies.

Electrochemical polymerization of a monomer initiated with the oxidation of monomer, this leads to the formation of resonance stabilized radical cation.(E)

Coupling takes place between either radical cation and monomer or two radical cations to form cation or dication, respectively. (C) Cation loses an electron to form a dication. Third step involves the loss of two protons so the formation of the neutral species. (E) Due to the extended conjugation of neutral dimer, it has lower oxidation potential than the monomer so dimer is oxidized preferentially. Either radical cation monomer or radical cation dimer meets with monomer or dimer to form trimer or tetramer. As polymerization proceeds, solubility decreases and oligomers precipitate out on the electrode. In order to continue depositing on the electrode, the neutral oligomers formed must be oxidized to the conducting form so that electrons can be transferred through the forming film to continue deposition.

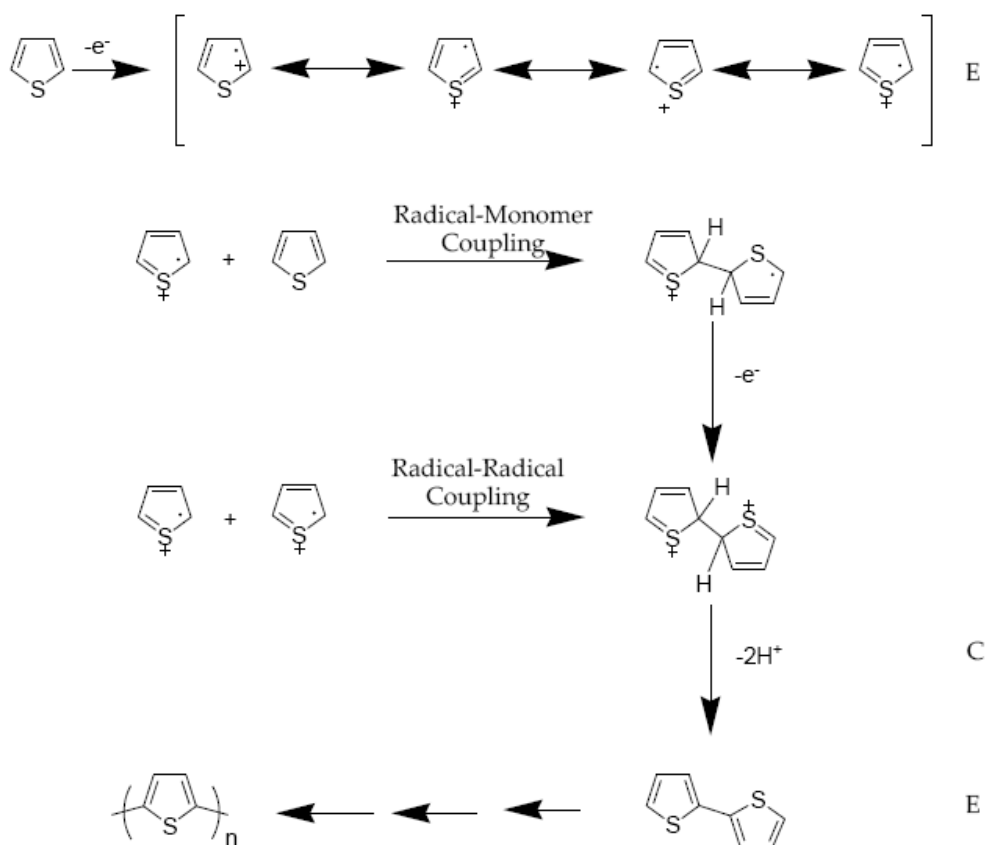


Figure 1.8 Electrochemical polymerization mechanism of thiophene

1.5.1.1 Thiophene Paradox

In electrochemical polymerization of thiophene, the potentials needed to oxidize thiophene monomer, is enough to overoxidize the polythiophene hence, polythiophene and overoxidized polythiophene are obtained together. Several solutions are proposed for this problem. Idea behind both of the solutions is the lowering the oxidation potential of the starting material. One is the use of thiophene oligomers which have lower oxidation potential. However, this solution has a drawback, conjugation length of the resultant polymer is low. Second solution is the use of β -substituted thiophenes which have lower oxidation potentials. In the literature 3-methylthiophene which has 0.2 V lower oxidation potential than thiophene itself, is used to overcome this problem [24].

1.5.2 Chemical Polymerization

Chemical polymerization can mainly be done via two ways; metal catalyzed coupling reactions and oxidative polymerization via FeCl_3 . Yamamoto, Suzuki and Stille coupling reactions are the commonly used metal catalyzed polymerizations. In the figure 1.9 reaction schemes for metal catalyzed coupling and chemical oxidation are shown.

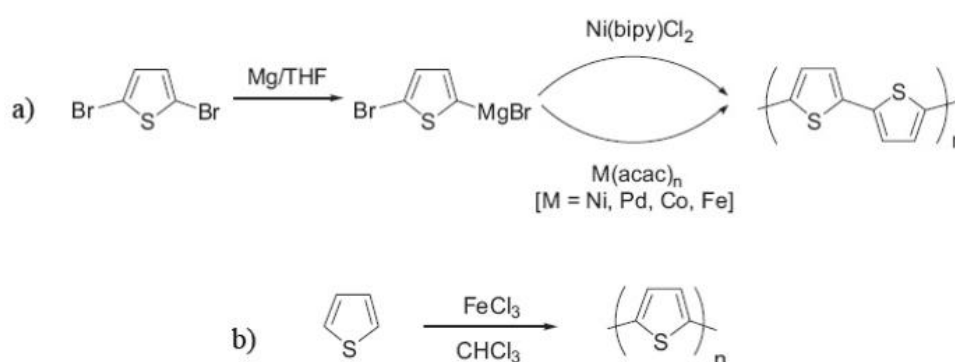


Figure 1.9 Synthesis of polythiophene via a) metal catalyzed coupling and b) chemical oxidation

1.6 Factors Affecting Band gap

The equation given below summarizes the factors affecting the band gap of conducting polymers. In order to control the band gap, bond length alternation ($E^{\Delta r}$), the mean deviation from planarity (E^{Θ}), the aromatic resonance energy (E^{res}), the inductive and mesomeric electronic effects of substituents (E^{sub}) and the interchain interactions (E^{Int}) should be taken into account [25].

$$E_g = E^{\Delta r} + E^{\Theta} + E^{\text{res}} + E^{\text{sub}} + E^{\text{Int}}$$

The figure below demonstrates the main factors influencing the band gap of conducting polymers.

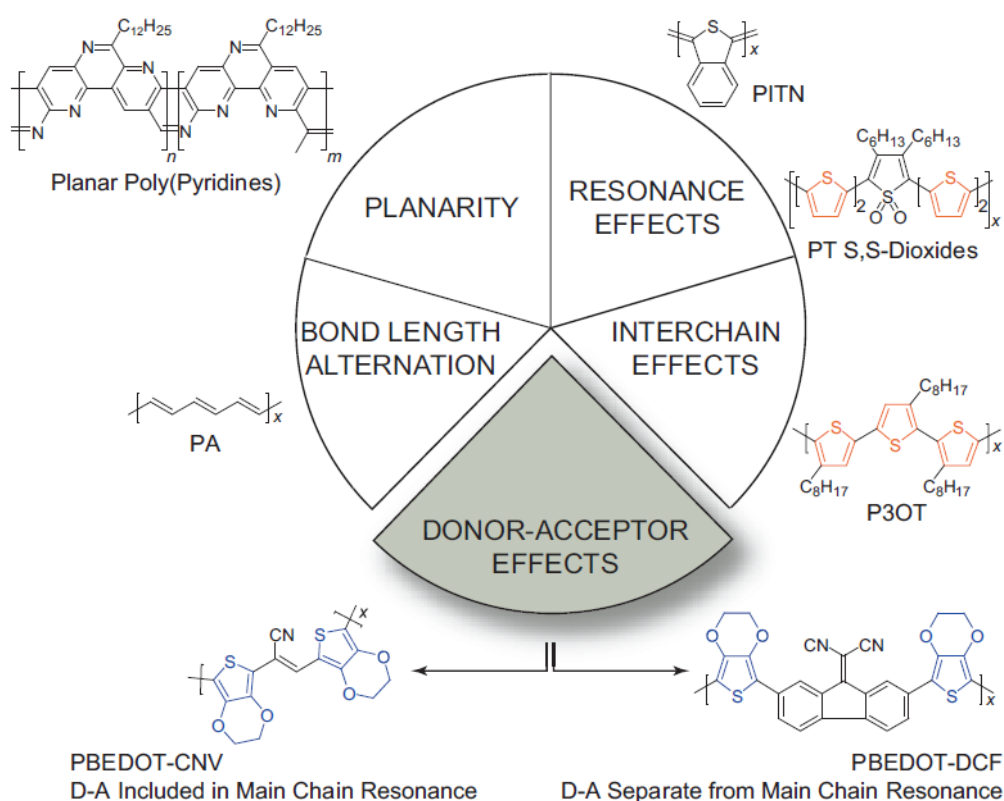


Figure 1.10 Overview of methods for the modification of band gap [26]

The most fundamental cause of a band gap in conjugated polymers is the bond length alternation. It is arising from the bond length difference between double and single bonds of conjugated systems. It is best envisioned as a competition between the nondegenerate quinoid and aromatic ground states represented in Figure 1-11. If the aromatic and quinoid forms of a conjugated polymer are energetically equivalent, they will be degenerate, and there will not be a competition between them, thus in principle, resultant polymer has zero band gap. Since polyacetylene has degenerate ground states, it is expected to have zero band gap, however it has band gap value of 1.4 eV because of the Peierls distortion [27].

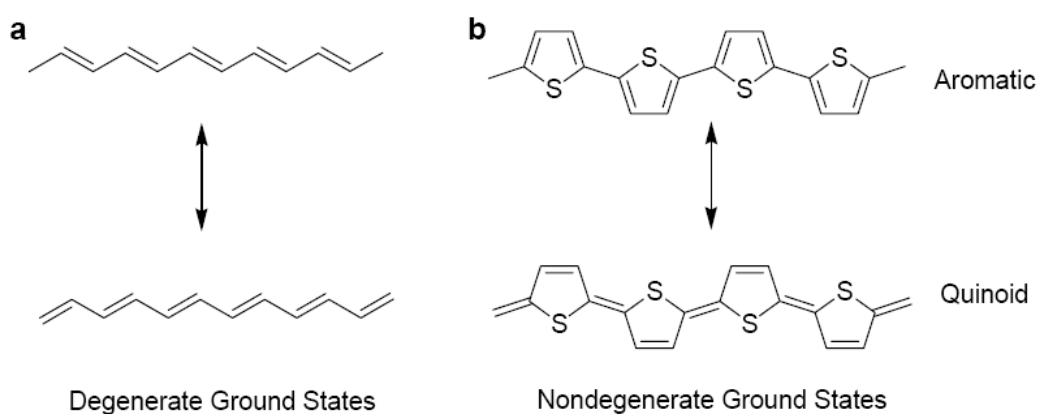


Figure 1.11 a) Illustration of degenerate ground state of polyacetylene,
 b) Illustration of non- degenerate ground state of polythiophene [28]

For aromatic polymers, synthetic efforts have been made to enhance the stability of the quinoid form relative to the aromatic form, with hopes of reducing the magnitude of the band gap. One important synthetic target has been the development of low band gap (or narrow band gap) conjugated polymers ($E_g \leq 1.5$ eV). As shown in the figure evolution of the polymer systems from polyacetylene to poly(BEDOT-Pyr) demonstrates the change of band gap via structural modification [29].

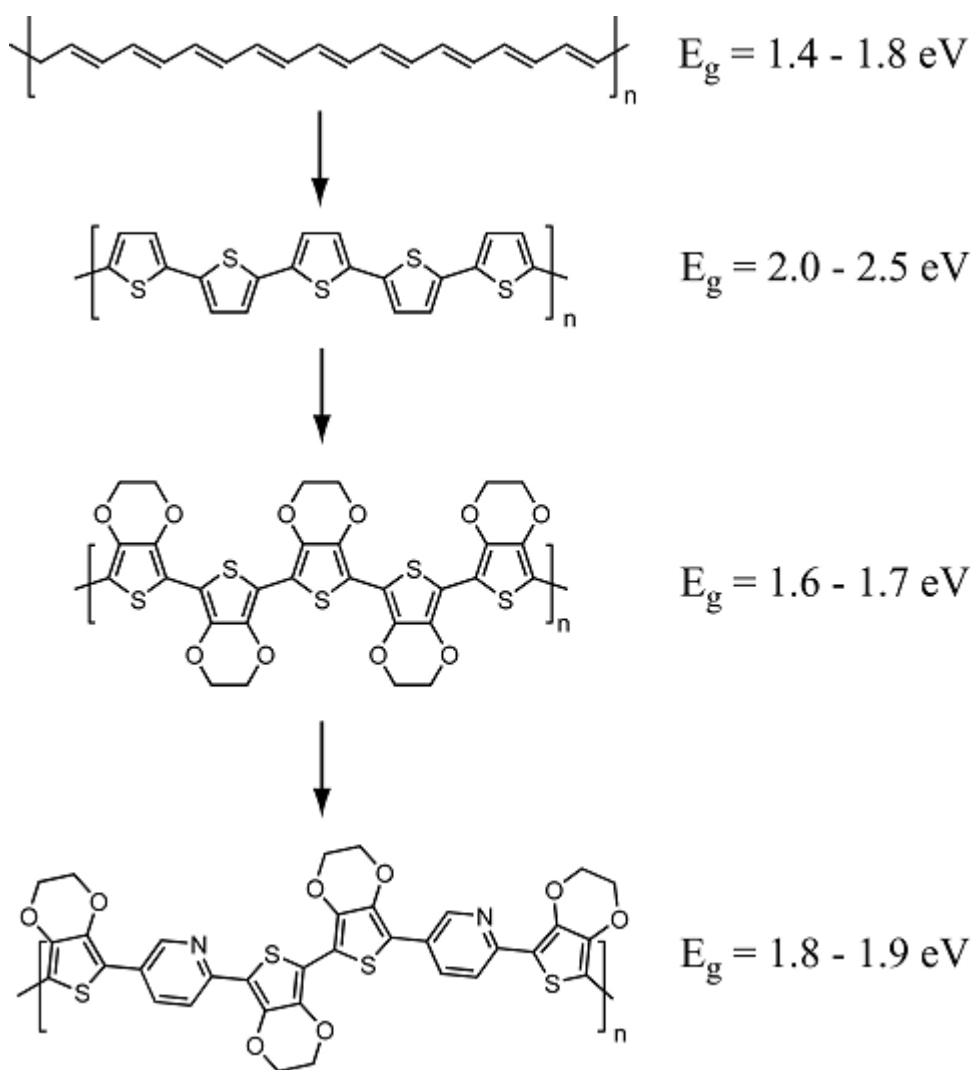


Figure 1.12 Evolution from polyacetylene to poly(BEDOT-Pyr)[29,30]

There are numerous synthetic strategies for tailoring the band gap of conjugated polymers to achieve the desired applications [31]. However, the donor-acceptor (DA) route, which provides electron rich and poor substituents on the polymer backbone, is the most utilized method in terms of the variety of synthetic possibilities. [31,32]

Benzothiadiazole [33,34], benzoquinoxalines [35], cyanovinylenes [36] thienopyrazines [37], perylenes [38] and benzotriazoles [39] have been used as effective acceptor units to achieve low band gap DA type polymers.

In this approach, the combination of an electron-rich donor and an electron-deficient acceptor in close conjugation results in a polymer with a reduced band gap. By carefully selecting the appropriate structure of the donor and the acceptor, band gap of the resultant polymer can be tuned.

In the figure 1.13, specific case of poly(bis-EDOT)-cyanovinylene (PBEDOT-CNV) is shown. It can be concluded that resultant polymer has HOMO energy close to the HOMO of the donor moiety, whereas it has LUMO energy close to the acceptor moiety. Therefore, band gap of the resultant polymer is lower than the parent donor and acceptor [40].

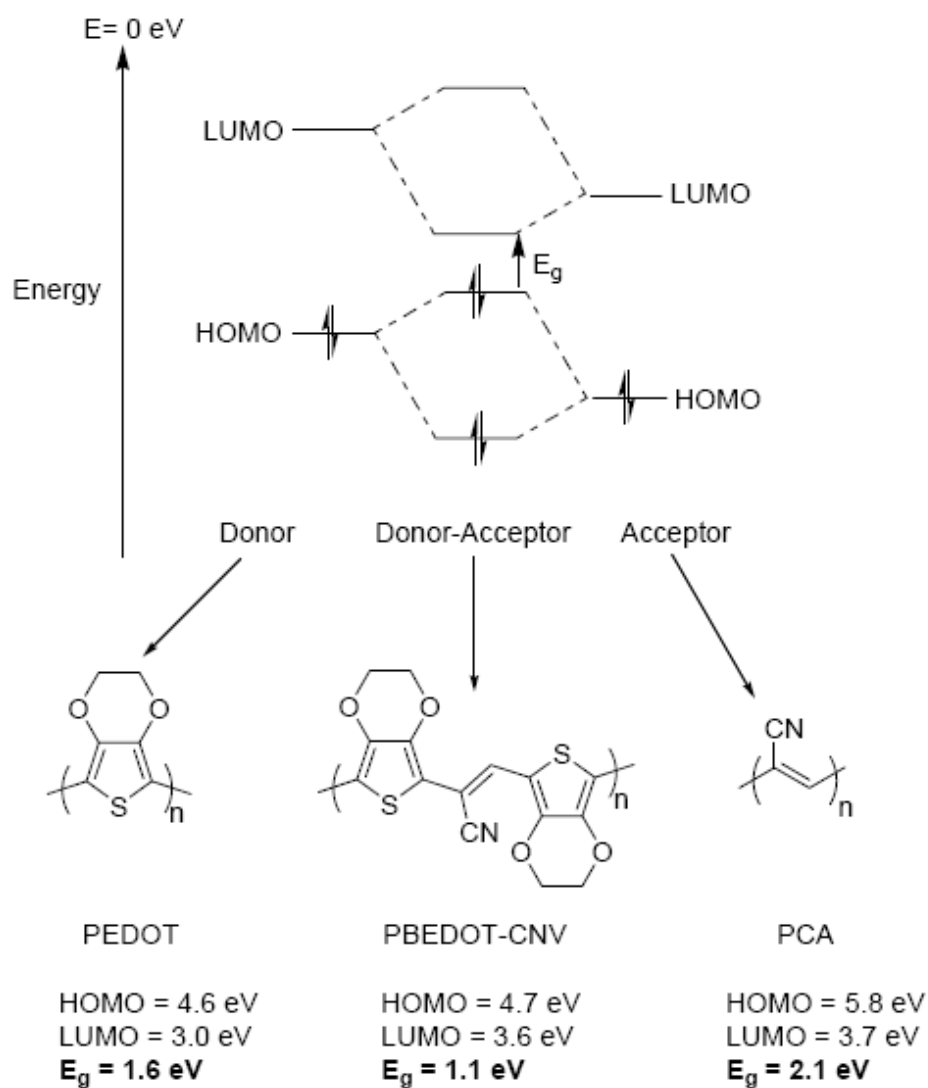


Figure 1.13 Schematic representation of the donor-acceptor approach to narrow band gap conjugated polymers [41]

1.7 Aim of This Work

As mentioned before with the discovery of conducting polymers, a new research area is opened and synthesis and electrochemical characterization of conducting polymers became a hot topic. Researchers from all over the world aim to synthesize polymers switching between all RGB (red- green- blue) colors, black and transmissive.

A polymer which shows all these properties was previously synthesized in our group. PTBT has tremendous optical properties. It shows all RGB colors, black and transmissive. It is soluble, fluorescent, processable, both p and n dopable. However it has quite high switching time [39b].

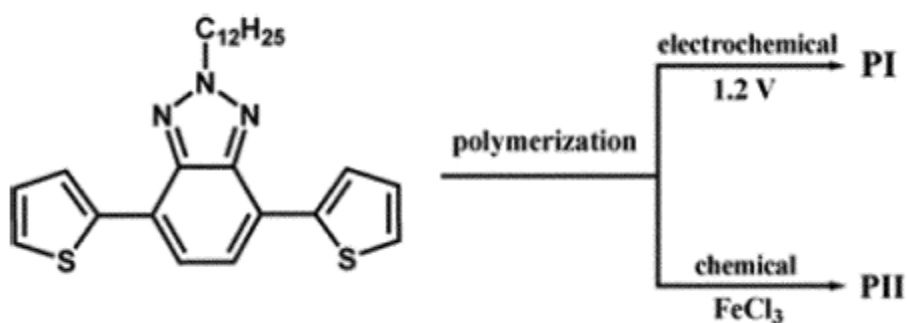


Figure 1.14 Structure of TBT and synthesis of PTBT

In this study, the aim is to synthesize polymers which also show tremendous optical properties like TBT with short switching times. Two benzotriazole based polymers were designed and their synthesis and electrochemical characterizations were carried out.

CHAPTER 2

EXPERIMENTAL

2.1 Materials

All chemicals were purchased from commercial sources and used without further purification unless otherwise mentioned. Methanol (MeOH) (Aldrich), ethanol (EtOH) (Aldrich), hexane (C₆H₁₄) (Aldrich), chloroform (CHCl₃) (Aldrich), dichloromethane (DCM) (Aldrich), bromine (Br₂) (Merck), hydrobromic acid (HBr, 47%) (Merck), n-butyllithium (n-BuLi, 2.5M in hexane) (Acros Organics), tributyltin chloride (Sn(Bu)₃Cl, 96%) (Aldrich), benzotriazole (Fluka), bromododecane (Aldrich), potassium tert-butoxide (K⁺(O*t*Bu)⁻) (Aldrich), thiophene (Aldrich), phenylenediboronic acid (Aldrich), bis(triphenylphosphine)palladium(II) dichloride (Aldrich) Tetrakis(triphenylphosphine)palladium(0) (Aldrich) were used as purchased. Prior to use, tetrahydrofuran (THF) (Fisher) was dried with sodium and benzophenone (Merck).

2.2 Methods

Tributyl(thiophene-2-yl)stannane [42] and 2-dodecyl-4,7-di(thiophen-2-yl)-2H-benzo[d][1,2,3]triazole (TBT) [39b] were synthesized according to previously described methods. PTBTPh was synthesized via Suzuki Coupling reaction whereas PTBTTh was synthesized via Stille Coupling reaction.

Suzuki coupling reaction takes place between dibromo monomer and diboronic acid or diboronic ester in the presence of Pd(0) catalyst. Since both water and toluene were used as the solvents $N(\text{Bu})_4\text{I}$ was used as the phase transfer catalyst. K_2CO_3 was the base; used to activate the boron for transmetalation with palladium.

In Stille Coupling reaction, dibromo compound was reacted with the distanylated compound in the presence of Pd(II) catalyst. Main drawback of the Stille coupling reactions is the low solubility of stanylated compound and the high toxicity of the tin compounds.

2.3 Equipment

All electrochemical studies were performed under ambient conditions using a Voltalab 50 potentiostat. ^1H and ^{13}C NMR spectra were recorded in CDCl_3 on a Bruker Spectrospin Avance DPX-400 Spectrometer. Electrochemical studies were performed in a three-electrode cell consisting of an indium tin oxide doped glass slide (ITO) as the working electrode, platinum wire as the counter electrode and an Ag wire as the reference electrode under ambient conditions. The value of normal hydrogen electrode (NHE) was taken as - 4.75 eV. Kinetic studies for the n-doped states were performed in dry acetonitrile purged with argon prior to use. ^1H and ^{13}C NMR spectra were recorded in CDCl_3 on a Bruker Spectrospin Avance DPX-400 Spectrometer. Chemical shifts were given in ppm downfield from tetramethylsilane. A Varian Cary 5000 UVVis spectrophotometer was used to perform the spectroelectrochemical studies of the polymer. Fluorescence measurements were conducted using a Varian Eclipse spectrofluorometer. Average molecular weight was determined by gel permeation chromatography (GPC) using a Polymer Laboratories GPC 220.

2.4 Procedure

2.4.1 Synthesis of 2-dodecylbenzotriazole

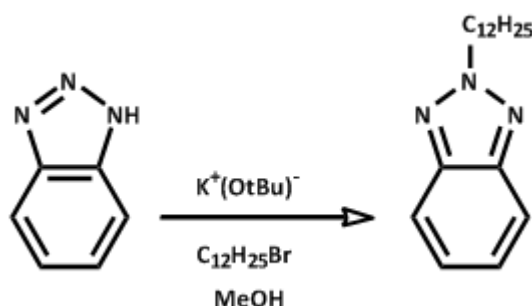


Figure 2.1 Synthesis of 2-dodecylbenzotriazole

Alkylation of benzotriazole was done according to previously published paper. [43] 5 grams of 1,2,3-benzotriazole (42 mmol), 12.2 grams of bromododecane (49 mmol) were refluxed in the presence of 5 grams of potassium tert-butoxide and 50 mL of methanol for 12 hours. After evaporation of the solvent, extraction with $CHCl_3$ and water was done. Organic phase was dried over $MgSO_4$ and solvent was dried. With column chromatography (3:2, chloroform:hexane), 3.7 grams of 2-dodecylbenzotriazole was obtained. 1H NMR (400MHz, $CDCl_3$, δ): 7.76 (m, 2H), 7.26 (m, 2H), 4.62 (t, $J=7.1Hz$ 2H), 2.12 (m, 2H), 1.25-1.15 (m, 18H), 0.78 (t, $J=6.0 Hz$, 3H); ^{13}C NMR (100MHz, $CDCl_3$, δ): 144.3, 126.1, 117.9, 56.6, 31.8, 30.0, 29.5, 29.4, 29.4, 29.3, 29.3, 29.0, 26.5, 22.6, 14.0.

2.4.2 Synthesis of 4,7-dibromo-2-dodecylbenzotriazole



Figure 2.2 Synthesis of 4,7-dibromo-2-dodecylbenzotriazole

To a two-necked round bottom flask, 3.7 grams of 2-dodecylbenzotriazole (13.1mmole) and 15 ml of HBr (47%) were added. Reaction mixture was heated at 100°C with stirring for 1 h. 5.9 grams of bromine (36 mmol) was added to mixture and it was refluxed for 12 hours at 135°C. After reaction has completed, mixture was treated with NaHCO₃ solution to get rid of excess Br₂. The residue was extracted with dichloromethane and brine. The combined organic layers were dried over MgSO₄ and concentrated under vacuum. The solid was then subjected to column chromatography (1:1, chloroform:hexane), affording 4.3 grams of 4,7-Dibromo-2-dodecylbenzotriazole. ¹H NMR (400MHz, CDCl₃, δ): 7.36 (s, 2H), 4.60 (t, J=7.0 Hz, 2H), 2.10 (m, 2H), 1.38-1.12 (m, 18H), 0.80 (t, J=6.9 Hz, 3H). ¹³CNMR (100 MHz, CDCl₃, δ): 143.7, 129.4, 109.9, 57.4, 31.8, 30.1, 29.5, 29.5, 29.4, 29.4, 29.3, 28.9, 26.4, 22.6, 14.0.

2.4.3 Synthesis of tributyl(thiophen-2-yl)stanne

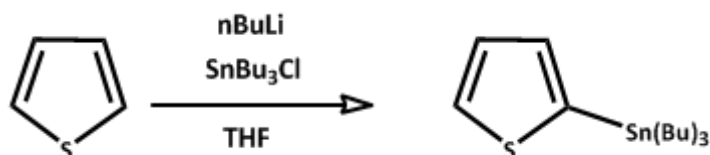


Figure 2.3 Synthesis of tributyl(thiophen-2-yl)stanne

A solution of thiophene (1g, 0.95 mL) in anhydrous THF (30 mL) was cooled to -78°C in a dry ice/acetone mixture under argon atmosphere. 5.76 mL of N-BuLi (2.5M) were added dropwise to the reaction mixture. After the addition was completed, reaction was stirred for 1.5 hours. Tributylstannyl chloride (3.48mL) was added slowly. Until the addition has completed temperature has kept constant at -78°C . After stirring the solution overnight at room temperature, solvent was evaporated to give the desired product. ^1H NMR (400MHz, CDCl_3 , δ): 7.69 (1H), 7.17 (1H), 7.00 (1H), 1.58, (6H), 1.30 (6H).1.31 (6H), 0.90 (9H)

2.4.4 Synthesis of 2,5-bis(tributylstannyl)thiophene

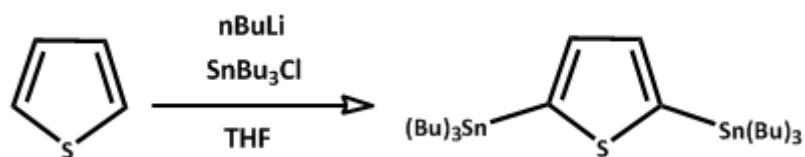


Figure 2.4 Synthesis of 2,5-bis(tributylstannyl)thiophene

Thiophene (2.1 g, 25 mmol) was dissolved in 20 mL dry THF under argon atmosphere. n-Butyl lithium (22 mL 2.5 M in hexane) was added drop wise at ambient temperature. The orange solution was heated under reflux for 45 min. The

resulting yellow suspension was cooled to room temperature and tributyltinchloride (18 g, 55 mmol) was added in one step and stirred overnight. Then THF was evaporated and the residue was extracted with CHCl_3 and water. The organic layer was collected and dried over MgSO_4 , the solvent was evaporated and 2,5-bis(tributylstannyl)thiophene was obtained after flash column chromatography (neutral alumina, hexane) as a colorless oily liquid. Yield 75%. ^1H NMR (400 MHz, CDCl_3 , d): 7.4 (s, 2H), 1.85 (m, 12H), 1.42 (m, 12H), 1.33 (m, 12H), 0.95 (m, 18H). ^{13}C {1H} NMR (100 MHz, CDCl_3 , d): 145.3, 139.1, 30.0, 29.5, 22.6, 14.0.

2.4.5 Synthesis of 2-dodecyl-4,7-di(thiophen-2-yl)-2H-benzo[d][1,2,3]triazole

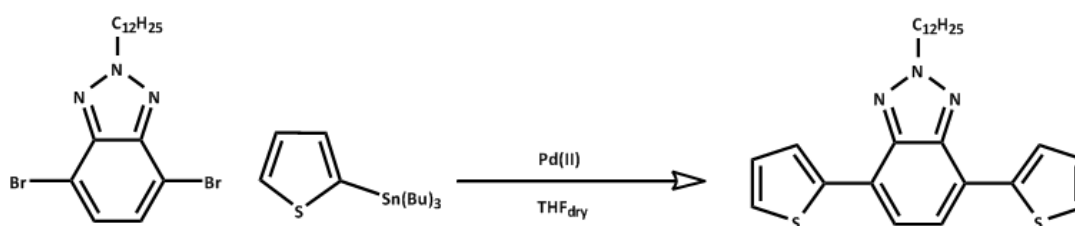


Figure 2.5 Synthesis of 2-dodecyl-4,7-di(thiophen-2-yl)-2H-benzo[d][1,2,3]triazole

4,7-Dibromo-2-dodecylbenzotriazole (100 mg, 0.224mmol) was dissolved in THF and tributyl(thiophen-2-yl)stannane were added at room temperature. Under argon atmosphere reaction mixture was heated to 110°C , then dichlorobis(triphenylphosphine)-palladium(II) (50 mg, 0.045 mmol) was added. The mixture was stirred overnight. THF was evaporated under vacuum and product (75mg) was obtained after column chromatography on silica gel ^1H NMR (400MHz, CDCl_3 , δ): 8.01 (d, $J=5.6$ Hz, 2H), 7.52 (s, 2H), 7.28 (d, $J=6.0$ Hz, 2H), 7.09 (t, $J_A=8.8$ Hz, $J_B=4.8$, 2H), 4.60 (t, $J=7.0$ Hz, 2H), 2.10 (m, 2H), 1.38-1.15 (m, 18H), 0.80 (t, $J=6.9$ Hz, 3H); ^{13}C NMR (100 MHz, DMSO-d_6 , δ): 142.4, 140.2, 128.4, 127.3, 125.8, 123.9, 123.0, 57.1, 32.2, 30.3, 29.9, 29.8, 29.7, 29.6, 29.5, 29.3, 26.9, 22.9, 14.4. MS (m/z): 451 [M $^+$]

2.4.6 Synthesis of 4,7-bis(5-bromothiophen-2-yl)-2dodecyl-2Hbenzo[d][1,2,3]triazole

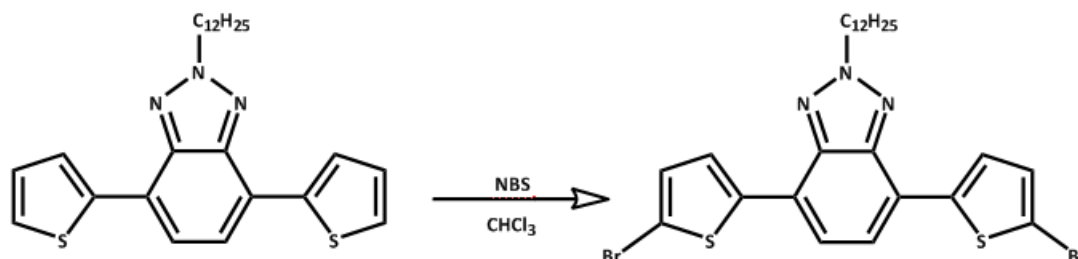


Figure 2.6 Synthesis of 4,7-bis(5-bromothiophen-2-yl)-2dodecyl-2Hbenzo[d][1,2,3]triazole

200 mg TBT (0.44 mmol) and 190 mg N-bromosuccinimide (1.07mmol) were stirred in 100 mL of CHCl₃ at room temperature in the dark. After 12 h, the solvent was removed under reduced pressure and the crude product was filtered over silica (eluent:CHCl₃) to obtain 250 mg (93%) **4** as yellow solid. ¹H NMR (400 MHz, CDCl₃, d): 7.72 (d, J $\frac{1}{4}$ 5.6 Hz, 2H), 7.44 (s,2H), 7.04 (d, J $\frac{1}{4}$ 6.0 Hz, 2H), 4.72 (t, J $\frac{1}{4}$ 7.0 Hz, 2H), 2.10 (m, 2H), 1.32–1.17 (m, 18H), 0.80 (t, J $\frac{1}{4}$ 6.9 Hz, 3H); ¹³C {¹H} NMR (100 MHz, DMSO-d₆, d): 144.4, 142.2, 140.4, 127.3, 125.8, 123.9, 123.0, 57.1, 32.2, 30.3, 29.9, 29.8, 29.7, 29.6, 29.5, 29.3, 26.9, 22.9, 14.4. MS (m/z): 608 [M⁺].

2.4.7 Synthesis of PTBTPh

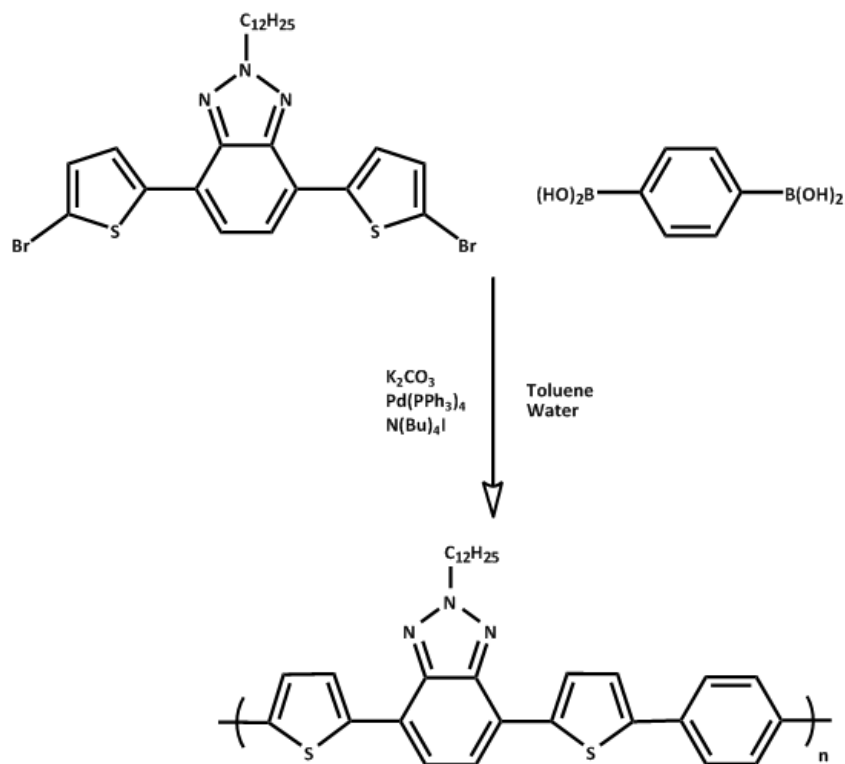


Figure 2.7 Synthesis of PTBTPh

4,7-bis(5-bromothiophen-2-yl)-2-dodecyl-1H-benzotriazole (1 mol equivalent) and 1,4-phenylenediboronic acid (1 mol equivalent), potassium carbonate (K_2CO_3 , 2 M in H_2O), toluene (3 : 2 toluene : water), $Pd(PPh_3)_4$ (5 mol%), and tetrabutylammonium iodide ($N(Bu)_4I$, 1 mol%) were refluxed under an argon atmosphere for 48 h. The solvent was removed and extracted with $CHCl_3-H_2O$ twice to remove the alkali solution. After combination of organic phases, the solvent was removed and the crude product was washed with methanol and acetone several times to obtain PTBTPh as a orange-red solid (140 mg, 56%). $M_n \frac{1}{4} 7000 M_w \frac{1}{4} 14800$, PDI $\frac{1}{4} 2.11$, $^1H NMR$ (400 MHz, $CDCl_3$, d): 8.00 (benzotriazole), 7.7 (thiophene), 7.6 (thiophene) 7.3 (benzene), 4.7 (N- CH_2), 2.1 (CH_2), 1.5–0.8 (pendant alkyl chain).

2.4.8 Synthesis of PTBTTh

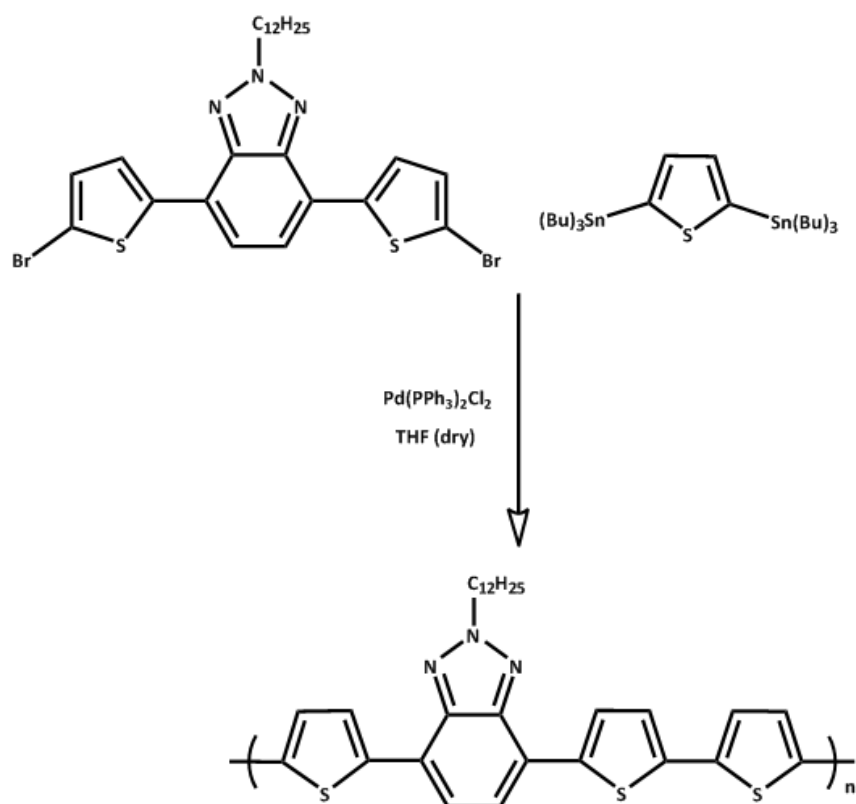


Figure 2.8 Synthesis of PTBTTh

4,7-bis(5-bromothiophen-2-yl)-2-dodecyl-1H-benzotriazole (1 mol equivalent) and 2,5-bis(tributylstannyl)thiophene (1 equivalent) were dissolved in anhydrous THF under an argon atmosphere and heated to reflux under argon. Pd(PPh₃)₂Cl₂ (5 mol%) was added under high argon flow. After 48 h of reflux to half of its initial volume the mixture was poured into 200 mL methanol. Precipitates were washed with methanol and acetone several times to give the PTBTTh as dark red solid. $M_n \approx 10000$ $M_w \approx 18000$, PDI ≈ 1.80 , ¹H NMR (400 MHz, CDCl₃, d): 8.00 (benzotriazole), 7.6 (thiophene), 7.4 (thiophene) 7.1 (thiophene), 4.7 (N-CH₂), 2.1 (CH₂) 1.5–0.8 (pendant alkyl chain).

2.5 Characterization of Conducting Polymers

2.5.1 Cyclic Voltammetry (CV)

Cyclic voltammetry is a very useful tool to investigate electroactivity of the monomers, to convert monomers into corresponding polymers and to determine the oxidation potential of the monomer and the redox potentials of the polymers. since in this study polymers were synthesized via chemical ways, cyclic voltammetry was used for determination of redox properties of the polymers.

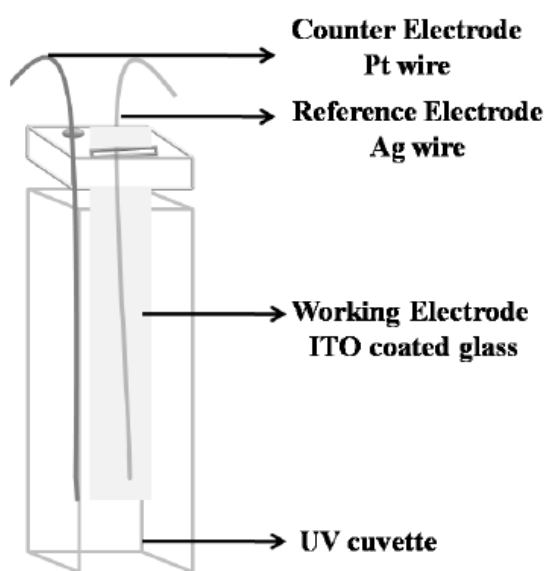


Figure 2.9 Demonstration of electrochemistry experiment set up

The polymers were dissolved in CHCl_3 and then spray coated on ITO glass electrodes. Counter, working and reference electrodes were connected to the Solartron 1285 potentiostat which applies the potential between working and reference electrode. Electrochemically inert solvent must be used. Most widely used solvent is acetonitrile due to its inertness in a wide range of potential

In this method, cycling potential is applied at a constant rate and resulting current is measured. The obtained data is a current density as a function of potential.

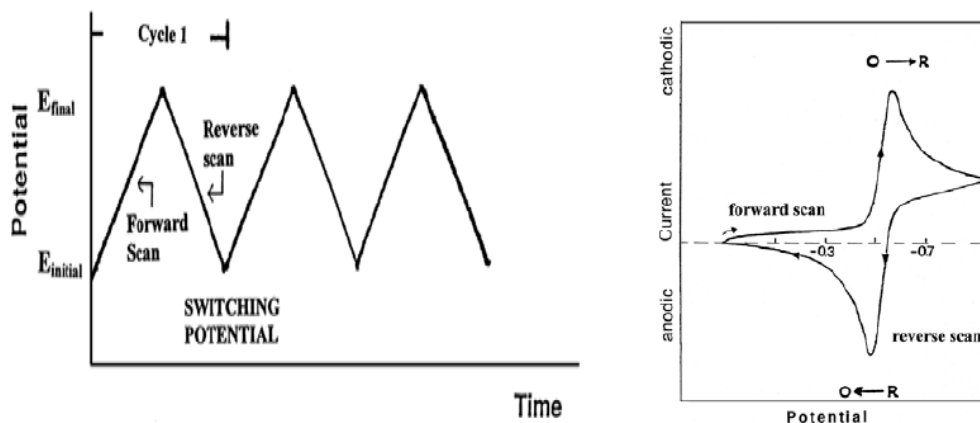


Figure 2.10 (a) Demonstration of applied potential as function of time
 (b) Demonstration of reversible oxidation reduction process

2.5.2 Spectroelectrochemistry

As mentioned before upon applied potential, color of conjugated polymers are changing due to the formation of new absorption bands. Formation of these new absorption bands can be probed by spectroelectrochemistry experiments. Spectroelectrochemistry is the combination of spectroscopic methods and the electrochemistry. In this method, first polymers were dissolved in CHCl_3 and then spray coated on ITO glass electrode. Electrodes were placed in UV cuvette and the evolution of the polymer absorption spectra is monitored as a function of applied potential.

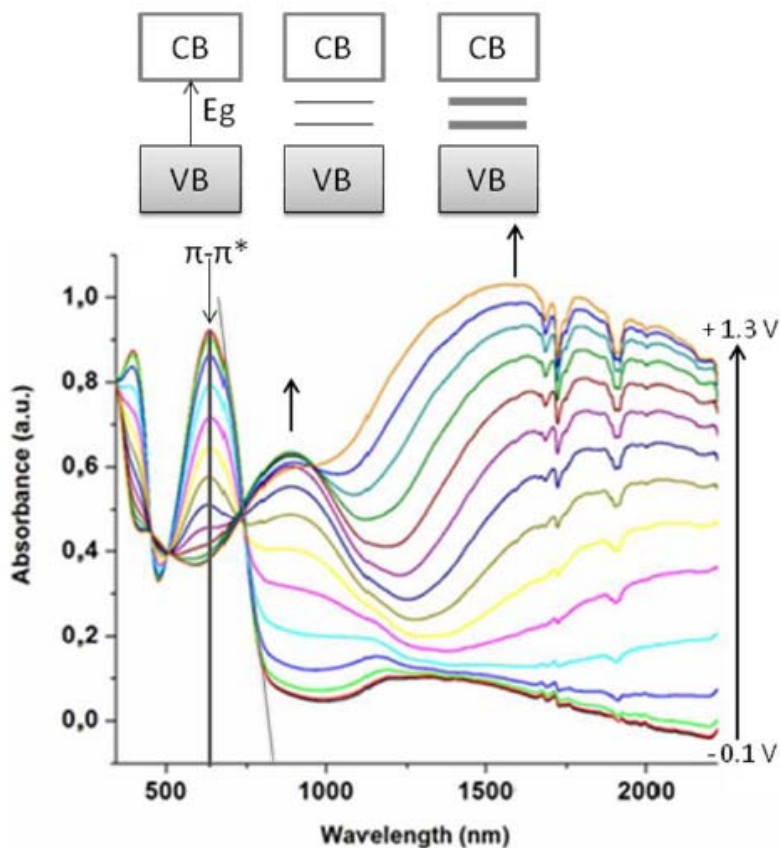


Figure 2.11 Spectra of a representative conducting polymer

2.5.3 Kinetic Studies

In order to monitor the optical contrast and switching time of polymers square wave potential step method coupled with optical spectroscopy is used. In this double potential step experiment the potential is set at an initial value for a set period of time and was then stepped to a second potential for a set period of time before being switched back to the initial potential. Meanwhile, percent transmittance (%T) of the polymer film is recorded.

The percent transmittance difference between oxidized and reduced state is defined as optical contrast ($\% \Delta T$). Switching time is the time required to oxidize the polymer from its reduced state.

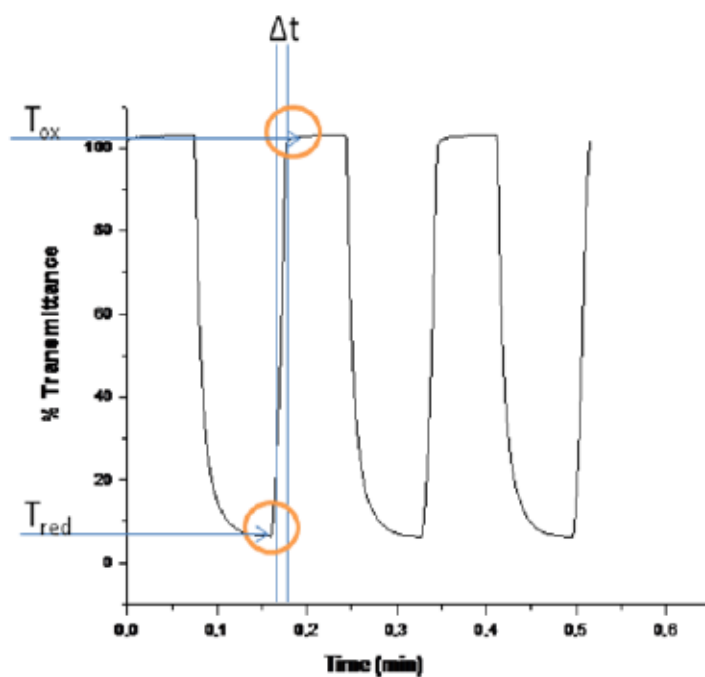


Figure 2.12 Kinetic study of a representative conducting polymer

CHAPTER 3

RESULTS AND DISCUSSION

3.1 Polymer Synthesis

Polymers shown in Figure 3.1 were synthesized by chemical cross coupling reactions, allowing for large scale production. High molecular weights are usually obtained via oxidative polymerization with FeCl_3 , whereas, palladium catalyzed polycondensation results in lower polydispersity, which has a significant effect on the order of the chains and the mobility of ions in the polymer in its thin film form [44]. In oxidative polymerization the final product is in its oxidized state, which is planar and mostly insoluble. This necessitates a long chemical reduction process in order to obtain soluble chains. On the other hand, a neutral state polymer can be achieved via polycondensation, where there is no need to de-dope the polymer chain before further characterizations, not to mention that this type of polymerization is suitable for industrial purposes. The polymer (PTBTPh) was synthesized via Suzuki coupling reaction between 4,7-bis(5-bromothiophen-2-yl)-2-dodecyl-2H-benzo[*d*][1,2,3]triazole and 1,4-phenylene diboronic acid and the polymer (PTBTTh) was synthesized via a Stille coupling reaction between 4,7-bis(5-bromothiophen-2-yl)-2-dodecyl-2H-benzo[*d*][1,2,3]triazole and 2,5-bis(tributylstannyl)thiophene. Gel permeation chromatography (GPC) results showed that number average molecular weights for the polymers were 7 kDa and 10 kDa for PTBTPh and PTBTTh, respectively with relatively low polydispersity indices (2.11 and 1.80).

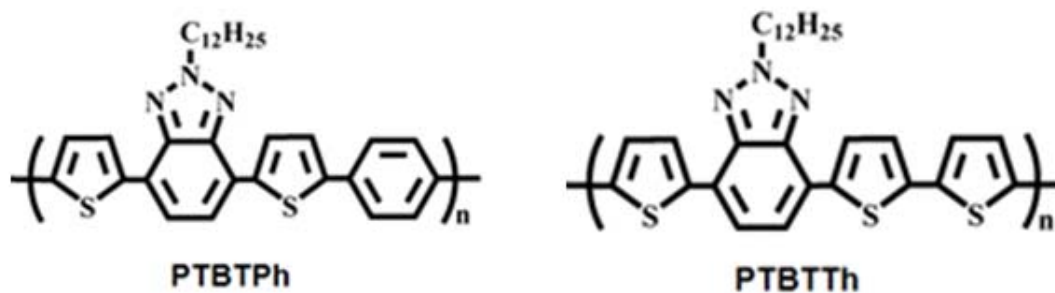


Figure 3.1 Chemical structures of PTBTPh and PTBTTh

3.2 Electrochemistry

For electrochemical characterization the polymers were dissolved in chloroform and then spray coated onto ITO coated glass slides. Once the solvent was evaporated, both of the polymers were subjected to cyclic voltammetry (CV).

3.2.1 Electrochemistry of PTBTPh

In order to determine the redox potentials of the PTBTPh in 0.1 M tetrabutylammonium hexafluorophosphate (TBAPF₆) was used as the electrolyte, acetonitrile (ACN) was used as the solvent. Potential was swept between 1.5 and -1.8V. The first run of PTBTPh resulted in a reversible redox couple at positive potentials peaked at 1.12 V and 0.75 V. The true n-type doping properties of the polymer was investigated by CV. PTBTPh was n-type dopable at negative potentials in combination with reversible doping/ dedoping peaks. Reduction of the PTBTPh film was achieved at -1.6 V and the reversible dedoping peak lies at -1.25 V as seen in Figure 3.2

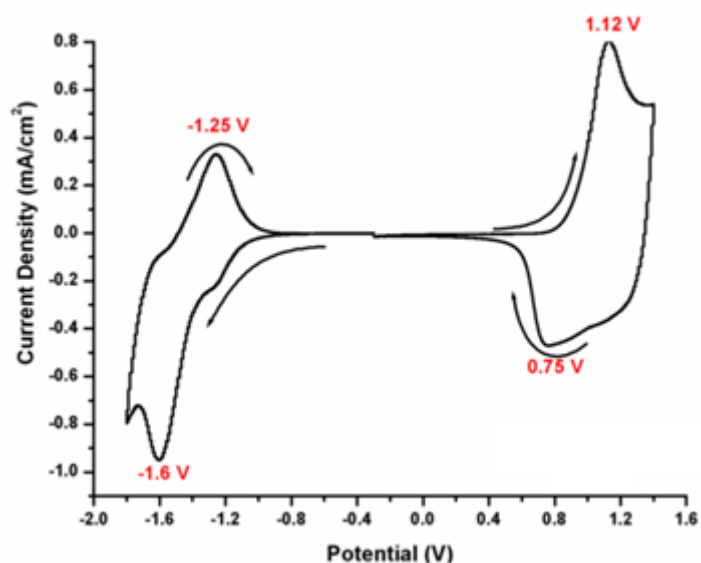


Figure 3.2 Cyclic voltammogram of PTBTPh

3.2.1 Electrochemistry of PTBTTh

Polymer film was subjected to cyclic voltammetry in order to determine the redox potentials of polymer in 0.1 M tetrabutylammonium hexafluorophosphate (TBAPF₆)/acetonitrile (ACN). The potential was swept between 1.5 V and -2.0 V for PTBTTh versus a Ag wire pseudo reference electrode. Due to the electron-rich thiophene units in the PTBTTh chains, the polymer film revealed lower redox potentials compared to those of PTBTPh (1.04 V and 0.64 V versus the same reference electrode). PTBTTh is also n-dopable. For PTBTTh, reduction was observed at (-1.89 V/ -1.56 V).

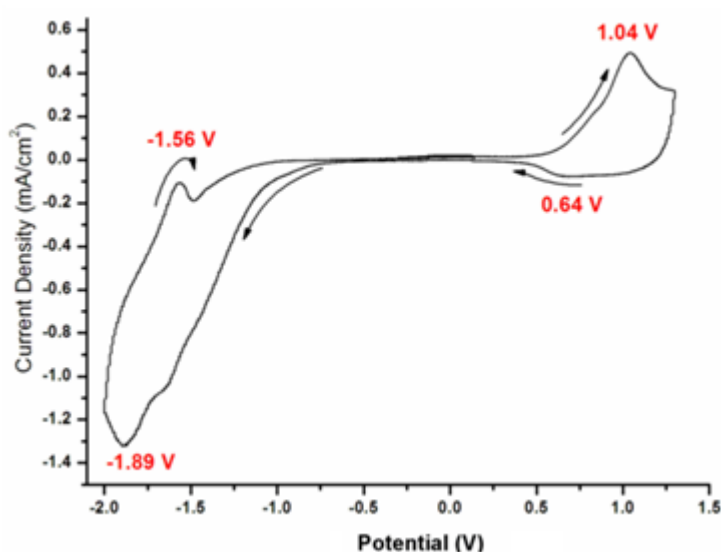


Figure 3.3 Cyclic voltammogram of PTBTTh

Due to the electron-rich thiophene units in the PTBTTh chains, the PTBTTh revealed lower redox potentials compared to those of PTBTPh. In addition to this, reduction of PTBTTh was observed at relatively higher potentials compared to PTBTPh, this is also due to the electron rich thiophene units in PTBTTh.

One common feature of these polymers is the accessibility of the n-doping at lower cathodic potentials, which makes the estimation of the LUMO possible.

Oxidation and reduction onset values were used to estimate the HOMO–LUMO energy levels of the polymers from the CV. The onset values were estimated by taking the intersection between the base line and the tangent line drawn to the increasing part of the current. The reference electrode and all the results were subsequently calibrated to Fc/Fc⁺ and the band energies were calculated relative to the vacuum level, considering that the value of NHE is -4.75 eV versus vacuum [45] and Fc/Fc⁺ 0.35 eV versus NHE, i.e., -5.1 eV versus vacuum. It is noteworthy to state that the energy levels were calculated precisely from CV due to the ambipolar property of the polymers. Table 3.1 summarizes the onset redox potentials, HOMO–LUMO energies and band gap values for the polymer films.

As seen from the table, additional electron rich thiophene units on PTBTTh eased the extraction of an electron from the polymer which corresponds to a higher HOMO and relatively low lying LUMO levels compared to its homologue. The electrochemical band gap values were calculated from the onset potentials as 2.15 eV and 1.80 eV for PTBTPh and PTBTTh, respectively.

Table 3.1 Electrochemical results, HOMO-LUMO energies and band gap values for PTBTPh and PTBTTh

	$E_{\text{onset}}^{\text{ox}}$ (V)	$E_{\text{onset}}^{\text{red}}$ (V)	HOMO (eV)	LUMO (eV)	E_g^{ec} (eV)	E_g^{op} (eV)
PTBTPh	0.85	-1.30	-5.95	-3.80	2.15	1.85
PTBTTh	0.65	-1.15	-5.75	-3.95	1.80	1.75

The electrochemical band gap values were calculated from the onset potentials as 2.15 eV and 1.80 eV for PTBTPh and PTBTTh, respectively. Calculated electrochemical band gaps were comparatively higher than the optical ones due to the creation of free ions in the electrochemical experiment (compared to a neutral excited state) [46]. The lower than expected value for PTBTTh may arise from the fact that this polymer is only slightly doped compared to PTBTPh. This can be evidenced from the current and charge values given in Figure 3.2 and 3.3

3.3 Spectroelectrochemistry

From the application point of view, spectroelectrochemical properties of the polymers should be evinced by electronic absorption spectra under applied potentials. Therefore, neutral **PTBTPh** and **PTBTTh** films were spray coated from a solution of polymers in chloroform and UV-vis-NIR spectra were recorded upon external bias. Spray coating was carried out until homogeneous films were achieved.

After solvent removal, the absorbance changes were noted as the potential was gradually increased between 0.0 V and 1.4 V in 0.1 M TBAPF₆/ ACN electrolyte-solvent couple.

3.3.1 Spectroelectrochemistry of PTBTPh

Absorbance changes for PTBTPh were noted while the potentials were increased from 0.0, to 0.6, 0.8, 0.95, 1.00, 1.05, 1.10, 1.15, 1.20, 1.25, 1.30, 1.35 and 1.40 V vs. Ag wire.

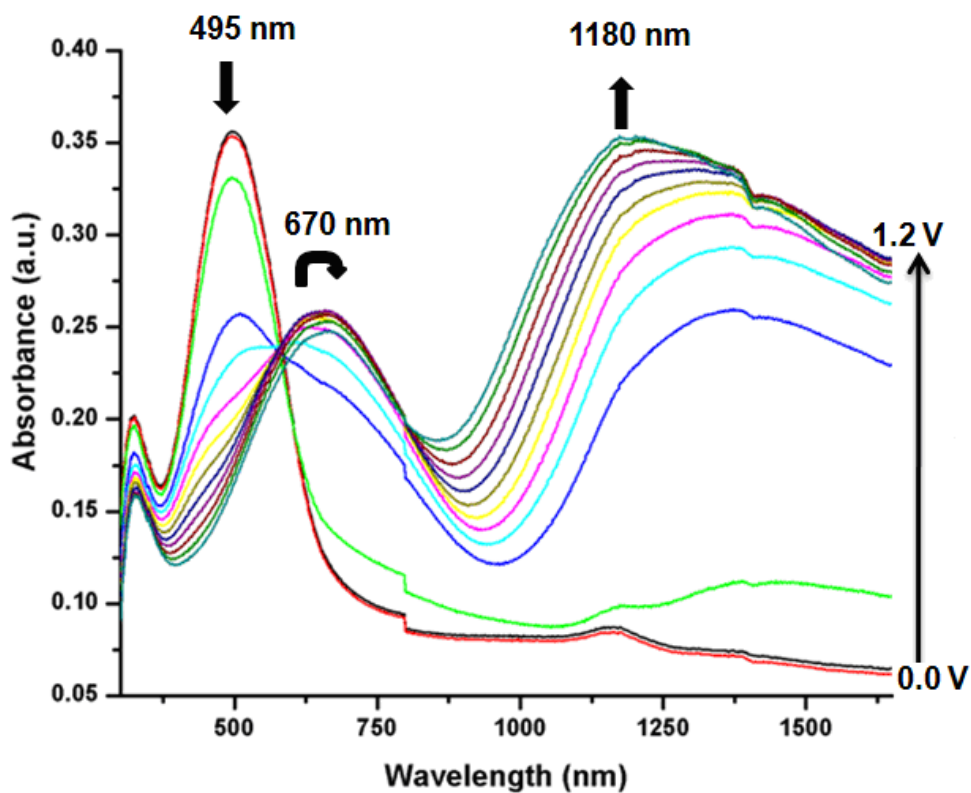


Figure 3.4 Spectroelectrochemistry studies of spray cast films of **PTBTPh**

3.3.2 Spectroelectrochemistry of PTBTTh

Absorbance changes for PTBTTh were noted while the potentials were increased from 0.0, to 0.1, 0.3, 0.5, 0.6, 0.7, 0.75, 0.775, 0.8, 0.825, 0.85, 0.875, 0.9, 0.925, 0.95, 0.975, 1.0, 1.025, 1.050, 1.075, 1.1, 1.15, 1.2, 1.25, 1.3, 1.35 and 1.4 V vs. Ag wire.

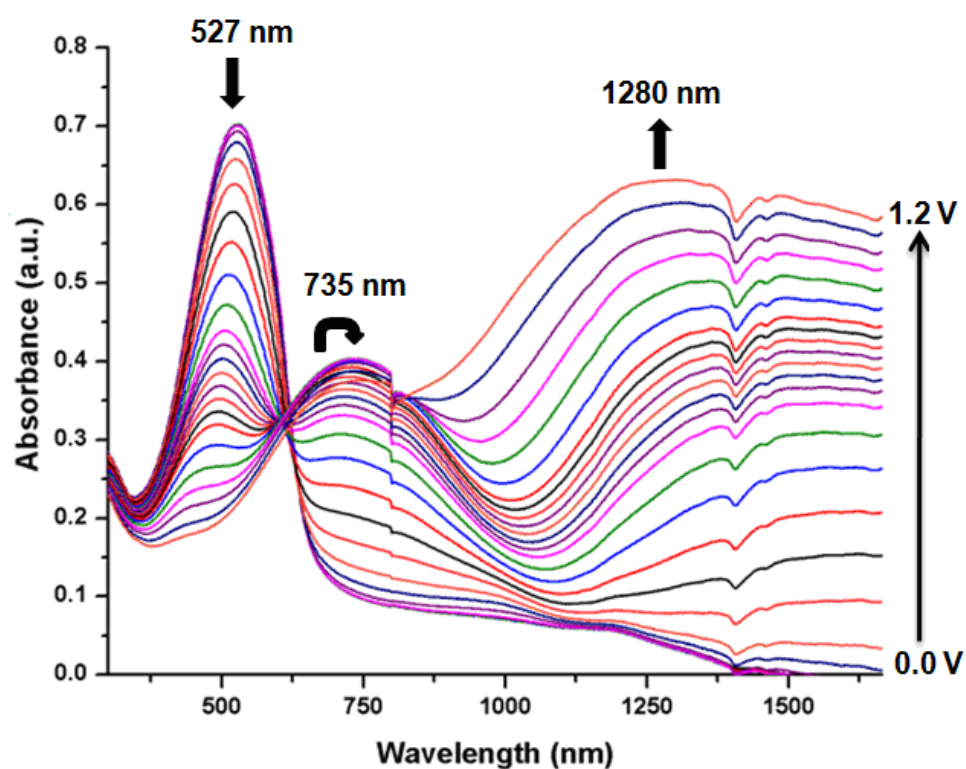


Figure 3.5 Spectroelectrochemistry studies of spray cast films of **PTBTTh**

PTBTPh has a dominant wavelength in the visible region centered at 495 nm with an absorption onset at 670 nm. Compared to **PTBTPh**, **PTBTTh** revealed a relatively red shifted maximum absorption in the visible region at 527 nm with an onset at 730 nm.

As potentials were increased, the absorptions in the visible region started to decrease simultaneously as the new bands were intensified in the NIR region at around 1180 nm and 1280 nm for **PTBTPh** and **PTBTTh**, respectively. The increased absorbance in the electronic absorption spectra of the polymer films in near-IR region indicates the formation of lower energy charge carriers such as polarons and bipolarons.

At early doping stages formation of polarons is followed by introduction of bipolarons with increased external bias. This trend is frequently been observed in π -conjugated polymers due to unfavorable bipolarons compared to polarons. However, max absorption in the NIR region for **PTBTPh** and **PTBTTh** corresponding to the bipolaronic states were increased simultaneously with polarons at low doping levels, which can be attributed to the presence of stable bipolaronic states on polymer backbone. Likewise, isosbestic points at around 600 nm for both the polymer films indicate the coexistence of more than one species [47].

Neutral and fully oxidized state absorption maxima of the polymer films in the visible were different by ca. 30-40 nm. Upon stepwise oxidation, four distinct colors were obtained from both polymers due to polaronic absorption bands located in the visible region. Phenyl unit instead of thiophene led to a less electron rich structure thus; λ_{max} for the neutral film was blue shifted by 32 nm resulted in orange-red color for **PTBTPh** whereas **PTBTTh** was red (Figure 3.6). This shift can also be attributed to the shorter soluble chains obtained for **PTBTPh** due to increased planarity and enhanced π - π interactions on polymer backbone. Additional substitution of phenyl and thiophene units compared to previously published polymer **PTBT** increased the doping rates of polymers and less color became detectable. Decreased distribution of benzotriazole moieties on polymer backbones allowed more accessible volume in the polymer films where dopant ions can be incorporated. This faster switching impeded the occurrence of two distinct transitions which is the main requirement to obtain green color in conjugated polymers.

Reduction of neutral polymer films resulted in depletion of optical absorption in the visible region and absorption of n-doped chains in NIR enabled highly transparent films in accessible potential range.

Partial oxidation of polymer films diminished the absorption intensity of neutral chains and when full visible absorption due to identical intensity of neutral and polaronic bands appeared, black color was observed. Upon fully doping of the polymer films at 1.2 V, both of the polymers exhibited strong absorption in the NIR region that supervened into the visible region so that the polymers were blue in their oxidized states due to the absorbance in the red region.

Both polymers were spray coated on ITO glass slides and placed in 0.1 M TBAPF₆/ACN solution, upon applied potential polymer films changed their color and the photographs were taken.

PTBTTh is red in its neutral state, upon applied potential it becomes purple, black and blue. When it is n-doped it becomes transparent. Whereas in its neutral state PTBTPh is orange upon oxidation it becomes brown black and blue. In its n-doped state it becomes transparent.

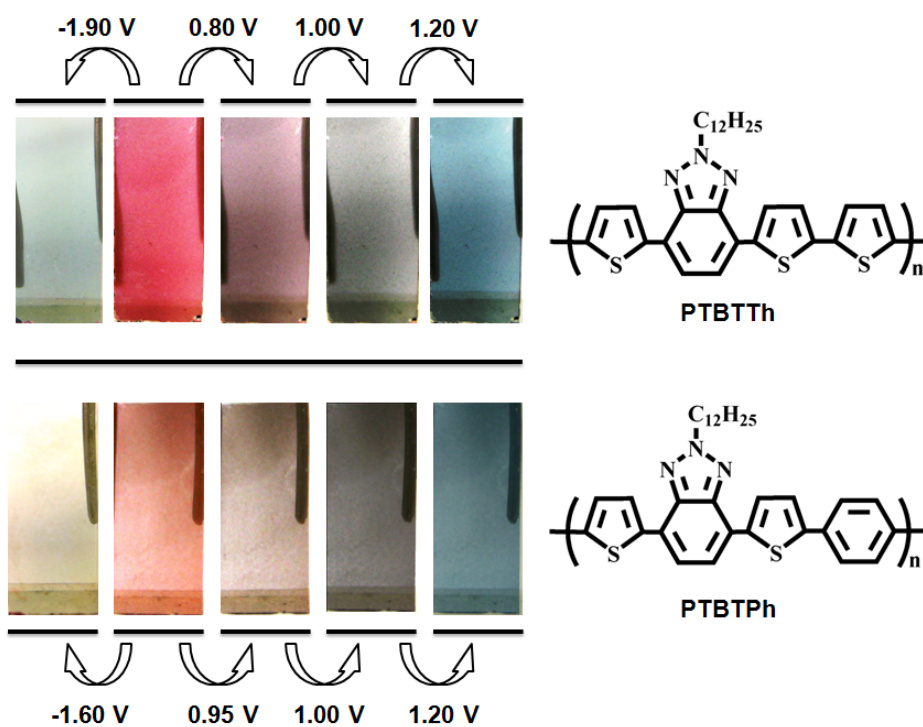


Figure 3.6 Spray coated **PTBTTh** (above) and **PTBTPh** (below) photographs in their neutral and fully oxidized states in 0.1 M TBAPF₆/ACN solution and the potentials where the corresponding colors were monitored.

3.4 Absorbance and Photoluminescence Studies of PTBTPh and PTBTTh

The absorbance spectra of **PTBTPh** and **PTBTTh** in both solution and thin film form, and photoluminescence (PL) spectra in CHCl₃ solution are shown in Figure 3.7. The lowest energy electronic transitions of solutions are centered at 476 and 494 nm for **PTBTPh** and **PTBTTh** respectively. Decreased conformational freedom, solvent-polymer interactions and tendency to aggregate in thin film form usually results in red shift absorption with respect to those taken in solution [48]. However, 20-32 nm red shifts for **PTBTPh** and **PTBTTh** represent the minority of aggregation and solvent-polymer chain interaction.

Additionally, long alkyl chains on the polymer backbone provide high solubility and the Stokes shifts were quite low when solutions were investigated in terms of their PL characteristics. Emission maxima of polymer solutions centered at 573 and 584 nm. Although, there is a very small difference between these emission maxima, **PTBTPh** was yellow whereas **PTBTTh** was orange under a standard UV lamp (366 nm) due to more intense shoulder at 618 nm. Both polymers revealed red-shifted emission compared to emission maxima for **PTBT** (Table 3. 2). Due to decreased number of alkyl chain per repeating unit in **PTBTPh** and **PTBTTh** lowered the solubility and the possible aggregate emission became more likely for these polymers.

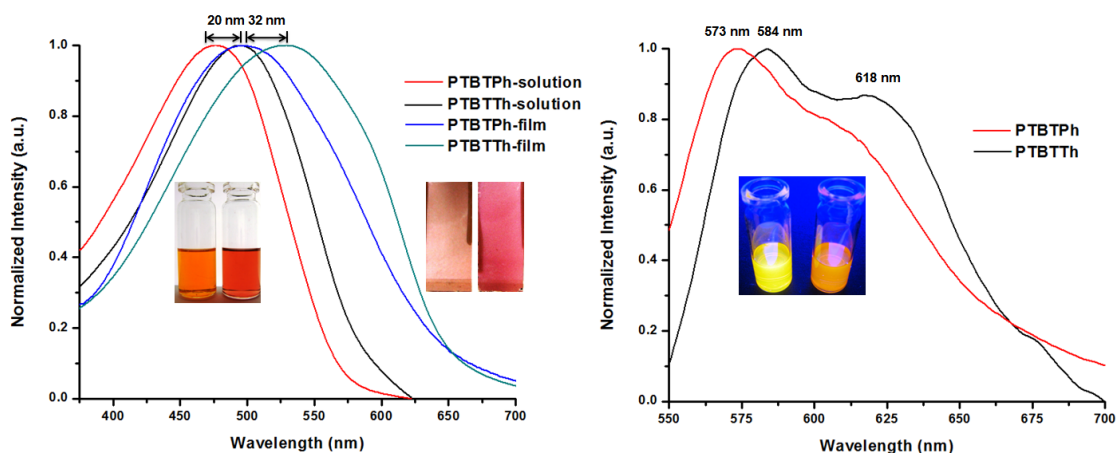


Figure 3.7 Solution and film absorbance spectra of **PTBTPh** and **PTBTTh** both in thin film form and solution and emission spectra of polymer solutions in chloroform

3.4 Kinetic Properties of **PTBTPh** and **PTBTTh**

Electrochromic switching studies were performed to monitor the percent transmittance changes as a function of time and to determine the switching times of the polymers at their λ_{\max} by stepping potentials repeatedly between their fully neutral and oxidized states (0.0 V and 1.2 V) within 5 s time intervals.

At its dominant wavelengths, **PTBTTh** revealed 40 % (527 nm) and 65 % (1280 nm) percent transmittance changes. **PTBTPh** showed lower optical contrast values compared to **PTBTTh** in visible and NIR region as 18 % (495 nm) and 30% (1180 nm), respectively. (Figure 5)

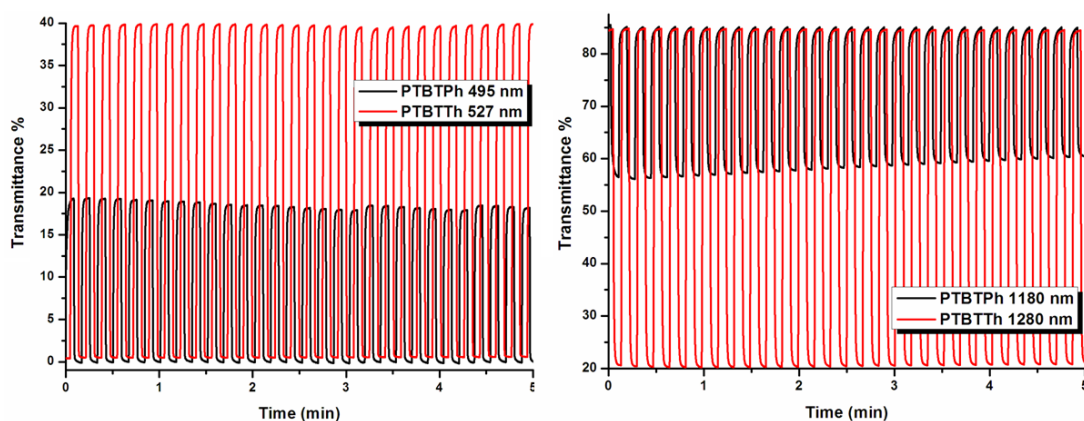


Figure 3.8 Percent transmittance changes by continuous monitoring at dominant wavelengths during switching between 0.0 V and 1.2 V in 0.1 M TBAPF₆/ ACN solution

In addition to transmittance changes upon doping/dedoping of a material, how quickly it reaches a full contrast is also crucial. Switching speed is defined as the time required for the polymer to attain its 95 % contrast value between its neutral (colored) and fully oxidized (bleached) states. In literature, 95 % of the full contrast and the corresponding switching times are used as the human eye is comparatively insensitive to 5% of change in color with little discerned between 95 % and full contrast (100 %). The times needed to reach 95 % of a full optical contrast between neutral and oxidized states and transmittance changes at dominant wavelengths for **PTBTPh**, **PTBTTh** and **PTBT** are given in Table 3.2

Table 3.2 Spectroscopic and optical results for polymers PTBTPh, PTBTTh, PTBTe (electrochemically synthesized) and PTBTc (chemically synthesized).^{*} Data obtained from 39b

	λ_{\max} film(nm)	λ_{\max} sln(nm)	λ_{\max} emm(nm)	Δ %T	t_{95} (s)
*PTBTe	503	447	542	35	2.4
*PTBTc	542	496	569	42	-
PTBTPh	495	475	573	18	1.6
PTBTTh	527	495	584	40	1.5

At 495 nm and 527 nm (which correspond to the dominant λ_{\max} values in the visible region), **PTBTPh** and **PTBTTh** switched between their neutral and oxidized states in 1.6 s and 1.5 s, respectively. Compared to **PTBT** (2.4 s), the switching times are shorter for these polymers due to included phenyl and thiophene units which led to interchain spacing that allows improved ion diffusion and dopant insertion. Nevertheless, improved switching times hindered the green color to be observable in **PTBTPh** and **PTBTTh** which was detected for **PTBT**.

CHAPTER 4

CONCLUSION

Two new DA type benzotriazole containing electrochromic polymers were synthesized via polycondensation and electrochemically characterized. Their electrochromic potential as multicolor to transparent materials were investigated. Results showed that these polymers can be used in non-emissive electrochromic applications and allow obtaining fine tuning in the color space due to their highly transmissive states. Kinetic properties such as optical contrasts (40% and 18%) and switching times (1.5 and 1.6 s) confirm their great candidacy. Moreover, these polymers can be used as back-light filter for white light with various colored and transmissive states. However, further investigation for these types of multicolored to transmissive, spray processable materials is necessary to improve their applications. From this perspective, design and synthesis of new materials are important for incorporation of them in industrial application.

This study was published in Journal of Materials Chemistry in 2011 [49].

REFERENCES

- [1] H. Shirakawa, E. J. Louis, A. G. MacDiarmid, C. K. Chiang, A. J. Heeger, *J. Chem. Soc., Chem. Commun.*, **1977**, 578.
- [2] Ö. Türkaslan, Msc Thesis, METU, **2006**.
- [3] H. Letheby, *J. Chem. Soc.* 15, **1862**, 161
- [4] S. Roth, *One-Dimensional Metals*, Weinheim VCH, **1995**
- [5] L.S. Hwang, J.M. Ko, H.W. Rhee, C.Y. Kim, *Synth. Met.* 55, **1993**, 3671.
- [6] J. Bobacka, *Anal. Chem.* 71, **1999**, 4932
- [7] (a) S. Gunes, H. Neugebauer and N. S. Sariciftci, *Chem. Rev.*, **2007**, 107, 1324–1338; (b) J. C. Bijleveld, A. P. Zoombelt, S. G. J. Mathijssen, M. M. Wienk, M. Turbiez, D. M. de Leeuw and R. A. J. Janssen, *J. Am. Chem. Soc.*, **2009**, 131, 16616–16617; (c) S. H. Park, A. Roy, S. Beaupre, S. Cho, N. Coates, J. S. M. D. Moses, M. Leclerc, K. Lee and A. J. Heeger, *Nat. Photonics*, **2009**, 3, 297–303; (d) A. P. Zoombelt, M. Fonrodona, M. M. Wienk, A. B. Sieval, J. C. Hummelen and R. A. Janssen, *Org. Lett.*, **2009**, 11, 903–906; (e) S. C. Price, A. C. Stuart and W. You, *Macromolecules*, **2010**, 43, 4609–4612.
- [8] (a) A. C. Grimsdale, K. L. Chan, R. E. Martin, P. G. Jokisz and A. B. Holmes, *Chem. Rev.*, **2009**, 109, 897–1091; (b) H. Tsuji, C. Mitsui, Y. Sato and E. Nakamura, *Adv. Mater.*, **2009**, 21, 3776–3779; (c) W. Y. Wong and C. L. Ho, *J. Mater. Chem.*, **2009**, 19, 4457–4482; (d) S. Beaupre, P. T. Boudreault and M. Leclerc, *Adv. Mater.*, **2010**, 22, E6–E27; (e) K. T. Kamtekar, H. L. Vaughan, B. P. Lyons, A. P. Monkman, P. Bryce and M. R Bryce, *Macromolecules*, **2010**, 43, 4481–4488.
- [9] (a) R. Mondal, H. A. Becerril, E. Verploegen, D. Kim, J. E. Norton, S. Ko, N. Miyaki, S. Lee, M. F. Toney, J. L. Bredas, M. D. McGhehee and Z. Bao, *J. Mater. Chem.*, **2010**, 20, 5823; (b) S. Allard, M. Forster, B. Souharce, H. Thiem and U. Scherf, *Angew. Chem., Int. Ed.*, **2008**, 1808 | (c) P. M. Beaujuge, W. Pisula, H. N.

- Tsao, S. Ellinger, K. Mullen and J. R. Reynolds, *J. Am. Chem. Soc.*, **2009**, 131, 7514–7515;
- (d) I. McCulloch, M. Heeney, C. Bailey, K. Genevicius, I. MacDonald, M. Shkunov, D. Sparrowe, S. Tierney, R. Wagner, W. Zhang, M. L. Chabinyc, R. J. Kline, M. D. McGehee and M. F. Toney, *Nat. Mater.*, **2006**, 5, 328–333; (e) L. L. Chua, J. Zaumseil, J. F. Chang, E. C. W. Ou, P. K. H. Ho, H. Sirringhaus and R. H. Friend, *Nature*, **2005**, 434, 194–199.
- [10] (a) G. Sonmez, H. B Sonmez, C. K. F. Shen, R. W. Jost, Y. Rubin and F. Wudl, *Macromolecules*, **2005**, 38, 669–675; (b) M. A. Invernale, Y. Ding, D. M. D Mamangun, M. S. Yavuz and G. A. Sotzing, *Adv. Mater.*, **2010**, 22, 1379–1382; (c) A. L. Dyer, M. L. Craig, J. E. Babiarz, K. Kiyak and J. R. Reynolds, *Macromolecules*, **2010**, 43, 4460–4467;
- [11] P. M. Beaujuge, S. V. Vasilyeva, S. Ellinger, T. D. McCarley and J. R. Reynolds, *Macromolecules*, **2009**, 42, 3694–3706; (e) A. Durmus, G. E. Gunbas, P. Camurlu and L. Toppare, *Chem. Commun.*, **2007**, 3246–3248; (f) G. E. Gunbas, A. Durmus and L. Toppare, *Adv. Mater.*, **2008**, 20, 691–695; (g) A. Bolduc, S. Dufresne and W. G. Skene, *J. Mater. Chem.*, **2010**, 20, 4820–4826
- [12] Salzner, U.; Lagowski, J. B.; Pickup, P. G.; Poirier, R. A. *Synth. Met.* **1998**, 96, 177-189
- [13] S.K. Deb and J.A. Chopoorian, *J. Appl. Phys.* **1968**, 37, 4818.
- [14] C.G. Granqvist, *Electrochim Acta*, **1999**, 44, 3005-3015
- [15] P. M. S. Monk, R. J. Mortimer and D. R. Rosseinsky, *Electrochromism: Fundamentals and Applications*, VCH, Weinheim, 1995
- [16] T. A. Skotheim and J. R. Reynolds, *Conjugated Polymers*, CRC Press, **2007**, 20-2
- [17] R.J. Mortimer, *Chem. Soc. Rev.*, **1997**, 26, 147-156
- [18] J. Roncali, *Chem. Rev.*, **1992**, 92, 711–738.
- [19] (a) C. L. Gaupp and J. R. Reynolds, *Macromolecules*, **2003**, 36, 6305–6315; (b) S. Varis, M. Ak, I. M. Akhmedov, C. Tanyeli and L. Toppare, *J. Electroanal. Chem.*, **2007**, 603, 8–14
- [20] C. J. DuBois and J. R. Reynolds, *Adv. Mater.*, **2002**, 14, 1844–1846.

- [21] A. Kraft, M. Rottman, H. D Gilsing and H. Faltz, *Electrochim. Acta*, **2007**, 52, 5856–5862.
- [22] C. Pozo-Gonzalo, M. Salsamendi, J. A. Pomposo, H. Grande, E. Y. Schmidt, Y. Y. Rusakov and B. A. Trofimov, *Macromolecules*, **2008**, 41, 6886–6894
- [23] H. K. Song, E. J. Lee and S. M. Oh, *Chem. Mater.*, **2005**, 17, 2232– 2233
- [24] B. Krische, M. Zagorska, *Synth. Met.* **1989**, 28, 263
- [25] J. Roncali, *Chem. Rev.*, **1997**, 97, 173–206.
- [26] C. A. Thomas, PhD Thesis, University of Florida, **2002**.
- [27] R.E. Peierls, *Quantum Theory of Solids*, Oxford University Press, **1955**
- [28] B. C. Thompson, PhD Thesis, University of Florida, **2005**
- [29] C. J. Dubois, PhD Thesis, University of Florida, **2003**
- [30] Roncali, *J. Chem. Rev.* **1997**, 97, 173-205
- [31] J. Roncali, *Chem. Rev.*, **1997**, 97, 173–206.
- [32] (a) U. Salzner and M. E. Kose, *J. Phys. Chem. B*, **2002**, 106, 9221– 9226; (b) A. Berlin, G. Zotti, S. Zechinn, G. Schiavon, B. Vercelli and A. Zanelli, *Chem. Mater.*, **2004**, 16, 3667–3676; (c) J. Roncali, *J. Mater. Chem.*, **1999**, 9, 1875–1893; (d) P. M. Beaujuge and J. R. Reynolds, *Chem. Rev.*, **2010**, 110, 268–320.
- [33] A. Durmus, G. E. Gunbas, P. Camurlu and L. Toppare, *Chem. Commun.*, **2007**, 3246–3248
- [34] 7 (a) D. Aldakov, M. A. Palacios and P. Anzenbacher, *Chem. Mater.*, **2005**, 17, 5238–5241; (b) P. Blanchard, J. M. Raimundo and J. Roncali, *Synth. Met.*, **2001**, 119, 527–528
- [35] (a) A. Durmus, G. E. Gunbas and L. Toppare, *Chem. Mater.*, **2007**, 19, 6247–6251; (b) G. E. Gunbas, A. Durmus and L. Toppare, *Adv. Funct. Mater.*, **2008**, 18, 2026–2030.
- [36] C. A. Thomas, K. Zong, K. A Abboud, P. J. Steel and J. R. Reynolds, *J. Am. Chem. Soc.*, **2004**, 126, 16440–16450
- [37] (a) B. P Karsten, L. Viani, J. Gierschner, J. Cornil and R. A. J. Janssen, *J. Phys. Chem. A*, **2009**, 113, 10343–10350; (b) G. Sonmez, C. K. F. Shen, Y. Rubin and F. Wudl, *Angew. Chem., Int. Ed.*, **2004**, 43, 1498–1502

- [38] E. Kozma, F. Munno, D. Kotowski, F. Bertini, S. Luzzati and M. Catellani, *Synth. Met.*, **2010**, 160, 996–1001
- [39] (a) A. Balan, G. Gunbas, A. Durmus and L. Toppare, *Chem. Mater.*, **2008**, 20, 7510–7513; (b) A. Balan, D. Baran, G. Gunbas, A. Durmus, F. Ozyurt and L. Toppare, *Chem. Commun.*, **2009**, 6768–6770; (c) G. A. Cetin, A. Balan, A. Durmus, G. Gunbas and L. Toppare, *Org. Electron.*, **2009**, 10, 34–41; (d) D. Baran, A. Balan, S. Celebi, B. M. Esteban, H. Neugebauer, S. Sariciftci and L. Toppare, *Chem. Mater.*, **2010**, 22, 2978–2987
- [40] A. L. Dyer, PhD Thesis, University of Florida, **2007**
- [41] R. N. Brookins, PhD Thesis, University of Florida, **2008**
- [42] S. S. Zhu and T. M. Swager, *J. Am. Chem. Soc.*, **1997**, 119, 12568–12577.
- [43] A. Tanimoto, T. Yamamoto, *Macromolecules*, **2006**, 39, 3546
- [44] P. Pingel, A. Achmad Zen, D. Neher, I. Lieberwirth, G. Wegner, S. Allard and U. Scherf, *Appl. Phys. A: Mater. Sci. Process.*, **2009**, 95, 67–72
- [45] E. R. Kötz, H. Neff and K. Müller, *J. Electroanal. Chem.*, **1986**, 215, 331–334
- [46] C. Q. Ma, M. Fonrodona, M. C. Schikora, M. M. Wienk, R. A. J. Janssen and P. Bauerle, *Adv. Funct. Mater.*, **2008**, 18, 3323–3331
- [47] K. A. Ashwini, A. Jenekhe and S. A. Jenekhe, *Chem. Mater.*, **1996**, 8, 579–589.
- [48] T. Q. Nguyen, I. B. Martini, J. Liu and B. J. Schwartz, *J. Phys. Chem. B*, **2000**, 104, 237–255.
- [49] G. Hizalan, A. Balan, D. Baran and L. Toppare, *J. Mat. Chem.*, **2011**, 21, 1804–1809

APPENDIX

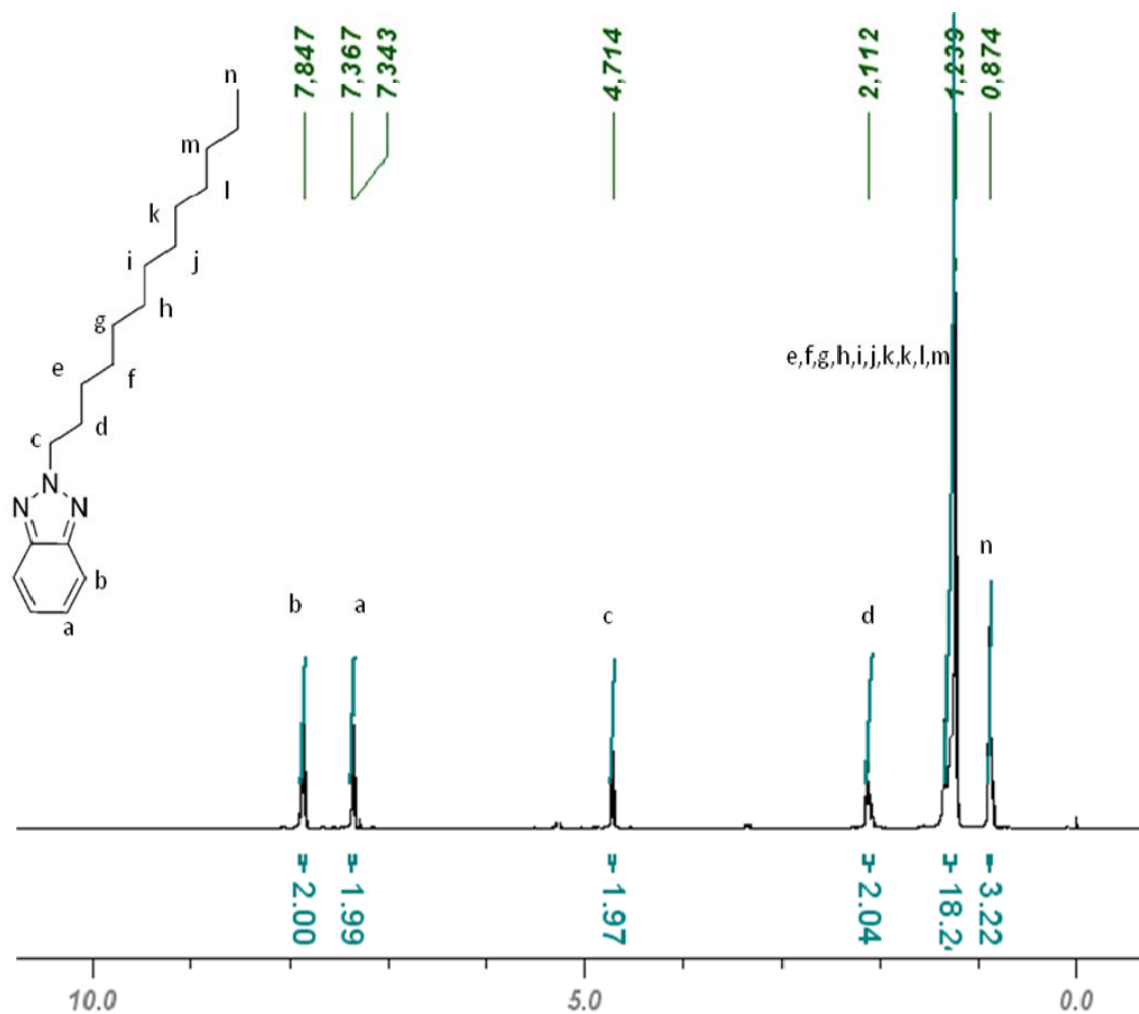


Figure A.1 ¹H-NMR spectrum of 2-dodecyl-2H-benzo[d][1,2,3]triazole

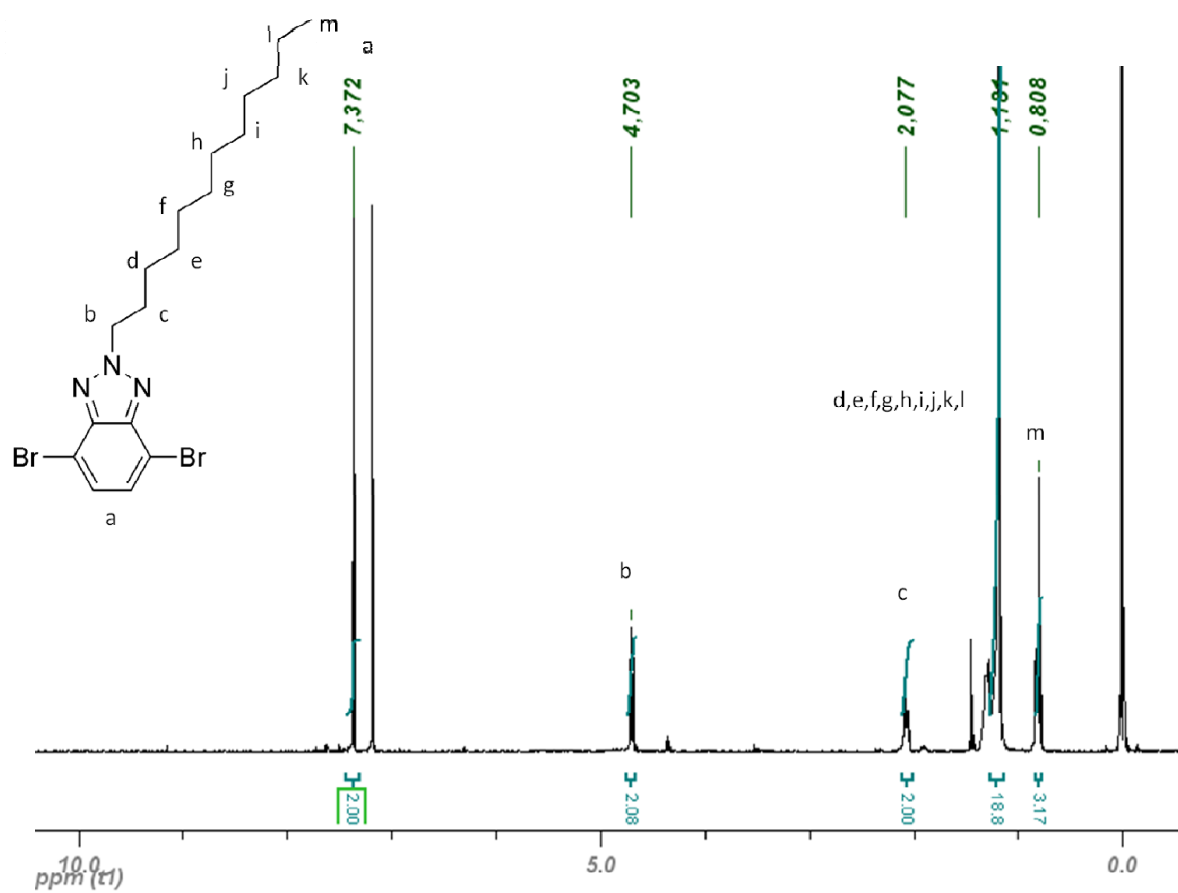


Figure A.2 ¹H-NMR spectrum of 4,7-dibromo-2-dodecyl-2H-benzo[d][1,2,3]triazole

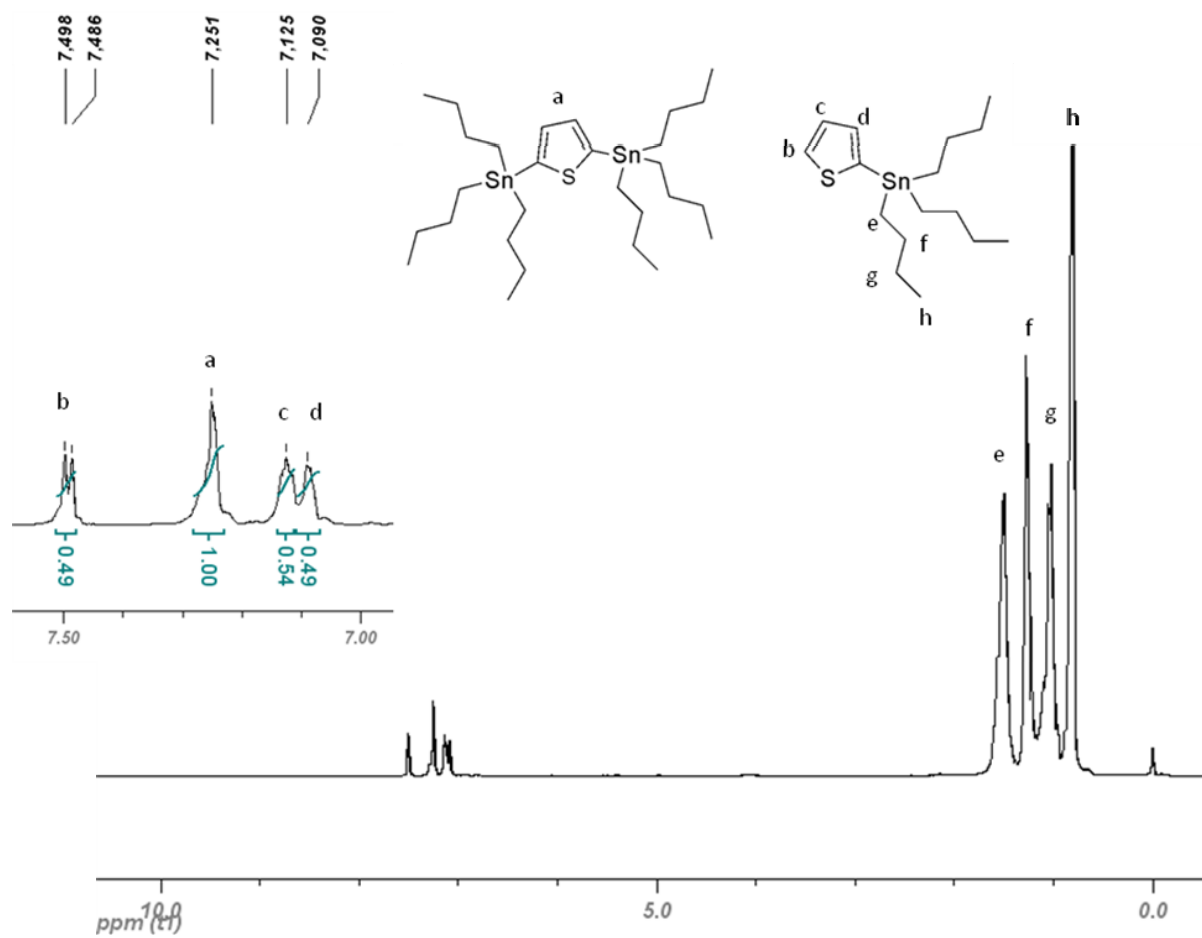


Figure A.3 $^1\text{H-NMR}$ spectrum of 2,5-bis(tributylstannyl)thiophene

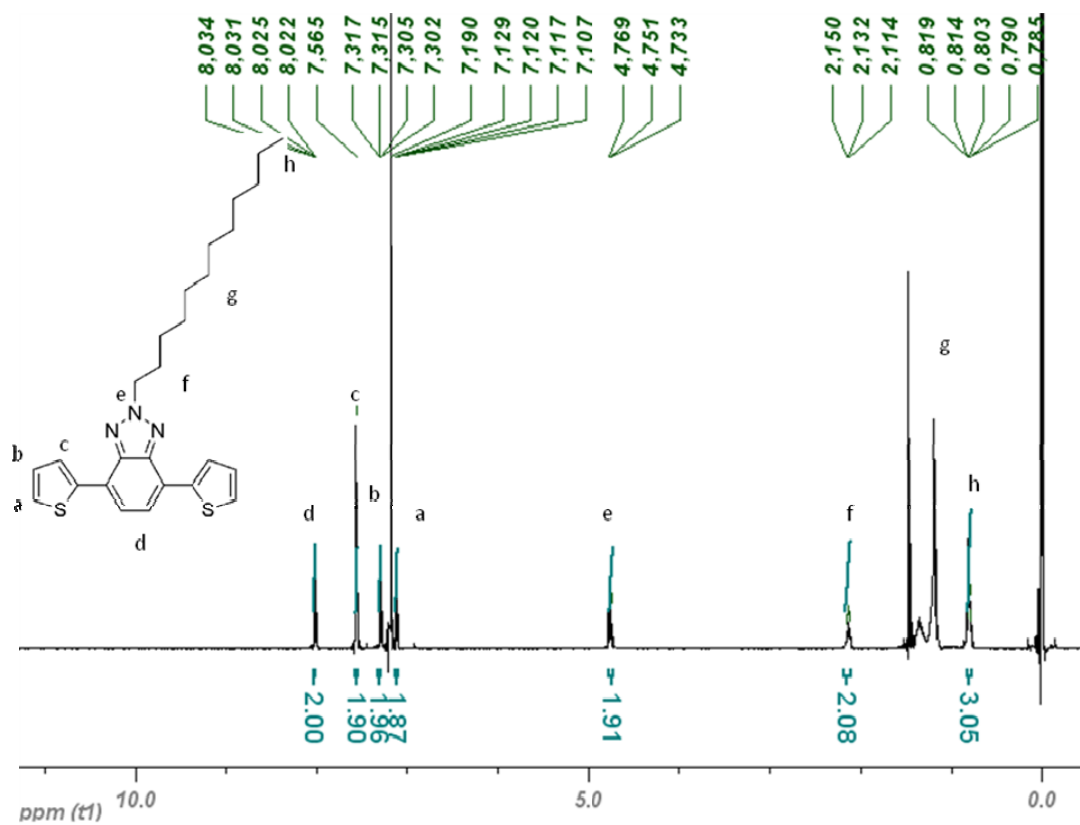


Figure A.4 ¹H-NMR spectrum of 2-dodecyl-4,7-di(thiophen-2-yl)-2H-benzo[d][1,2,3]triazole

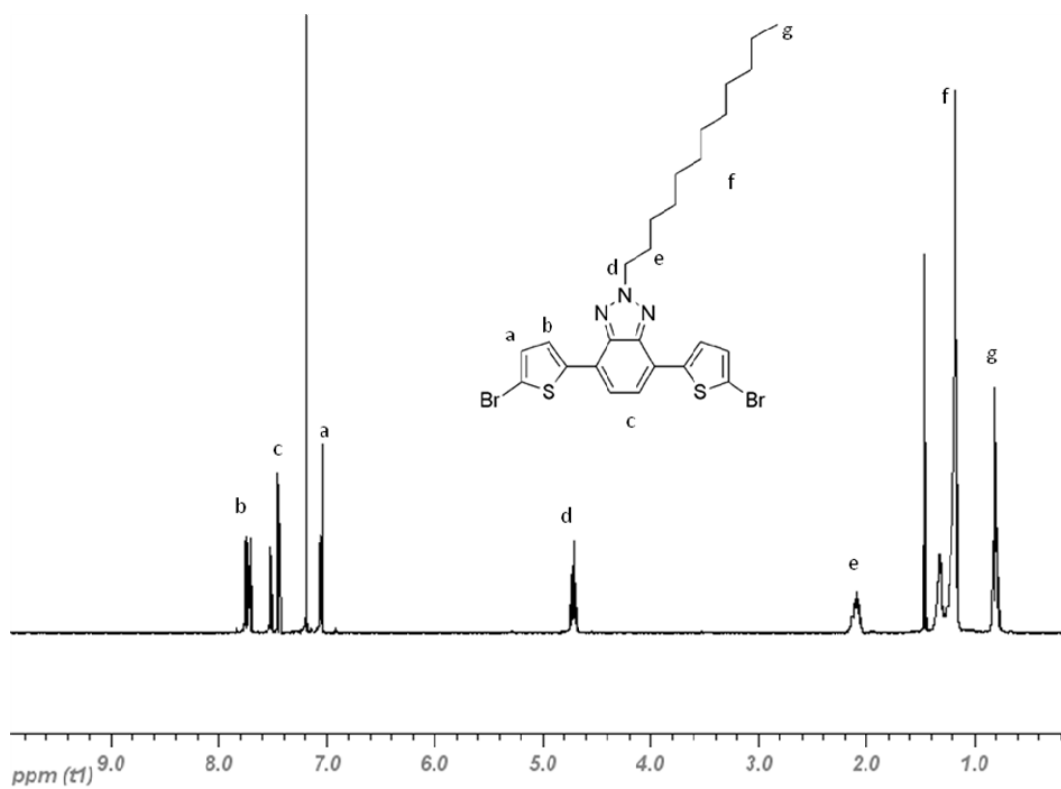


Figure A.5 $^1\text{H-NMR}$ spectrum of 4,7-bis(5-bromothiophen-2-yl)-2-dodecylbenzo[d][1,2,3] triazole

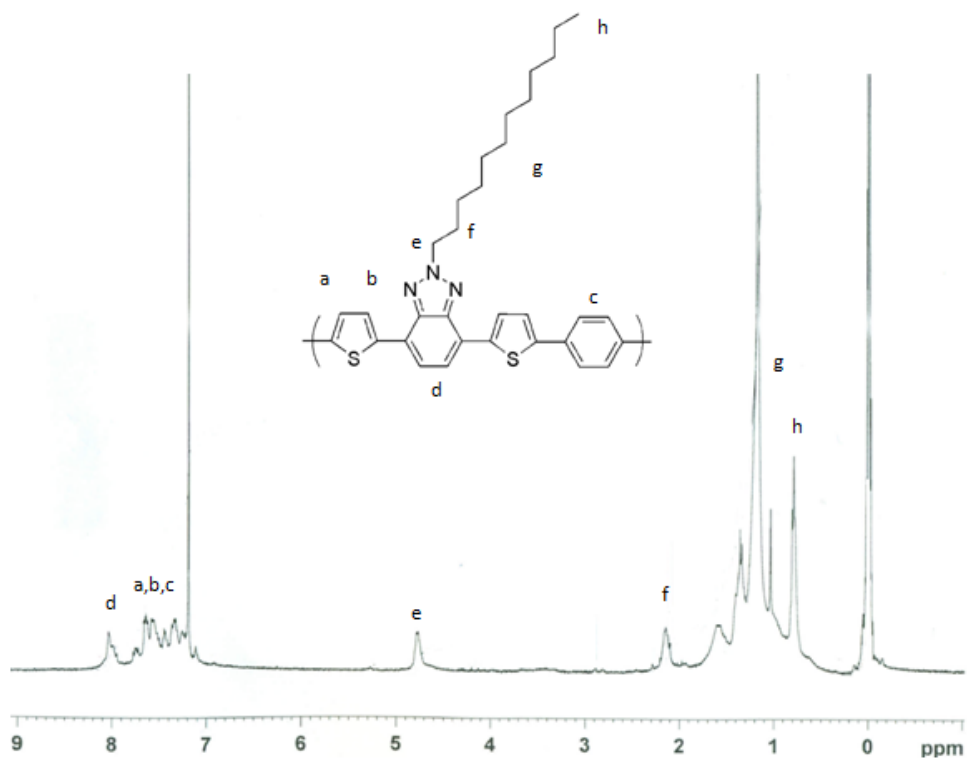


Figure A.6 ¹H-NMR spectrum of PTBTPh

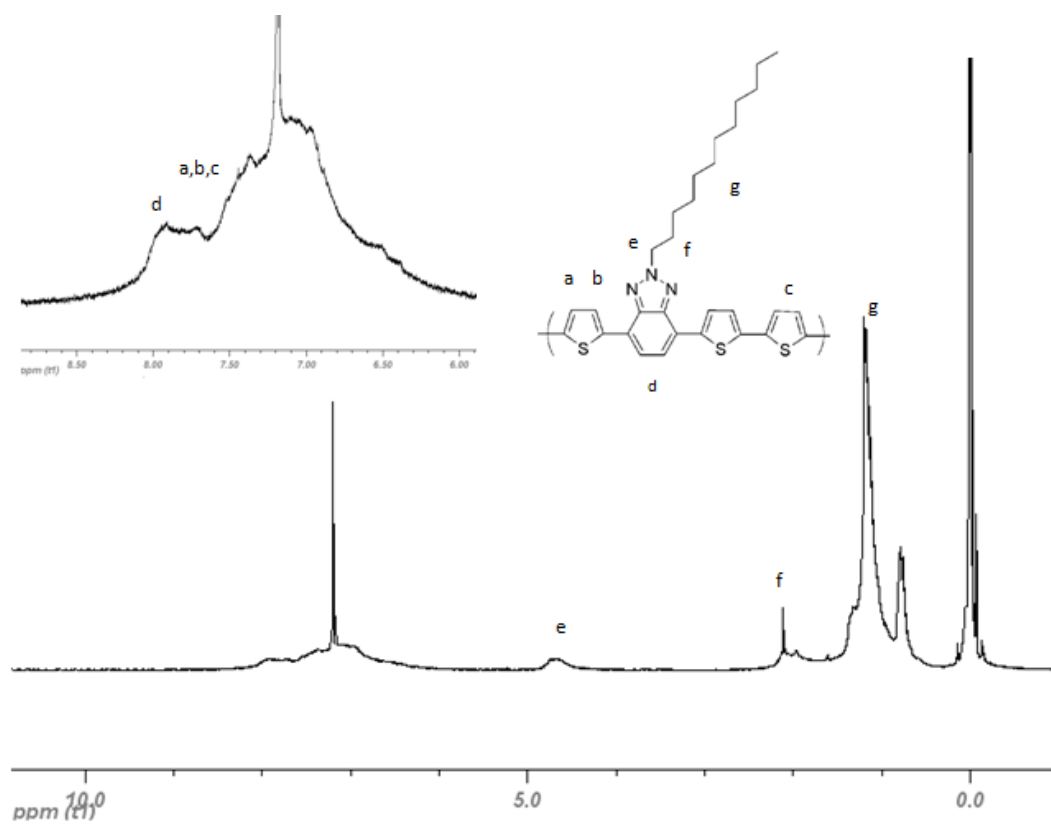


Figure A.7 $^1\text{H-NMR}$ spectrum of PTBTTh